Mathematical models in population dynamics and ecology

Rui DILÃO

Institut des Hautes Études Scientifiques

35, route de Chartres

91440 – Bures-sur-Yvette (France)

Juin 2004

IHES/M/04/26

CHAPTER 15

MATHEMATICAL MODELS IN POPULATION DYNAMICS AND ECOLOGY

Rui Dilão

Non-Linear Dynamics Group, Instituto Superior Técnico
Av. Rovisco Pais, 1049-001 Lisbon, Portugal
and
Institut des Hautes Études Scientifiques
Le Bois-Marie, 35, route de Chartres, F-91440 Bures-sur-Yvette, France
E-mail: rui@sd.ist.utl.pt

We introduce the most common quantitative approaches to population dynamics and ecology, emphasizing the different theoretical foundations and assumptions. These populations can be aggregates of cells, simple unicellular organisms, plants or animals.

The basic types of biological interactions are analysed: consumer-resource, prey-predation, competition and mutualism. Some of the modern developments associated with the concepts of chaos, quasi-periodicity, and structural stability are discussed. To describe short- and long-range population dispersal, the integral equation approach is derived, and some of its consequences are analysed. We derive the standard McKendrick age-structured density dependent model, and a particular solution of the McKendrick equation is obtained by elementary methods. The existence of demography growth cycles is discussed, and the differences between mitotic and sexual reproduction types are analysed.

Contents

1. Introduction

In a region or territory, the number of individuals of a species or a community of species changes along the time. This variation is due to the mechanisms of reproduction and to the physiology of individuals, to the resources supplied by the environment and to the interactions or absence of interactions between individuals of the same or of different species.

Biology is concerned with the architecture of living organisms, its physiology and the mechanisms that originated life from the natural elements. Ecology studies the relations between living organisms and the environment, and, in a first approach, detailed physiological mechanisms of individuals have a secondary importance.

As a whole, understanding the phenomena of life and the interplay between living systems and the environment make biological sciences, biology together with ecology, a complex science. To handle the difficulties inherently associated to the study of living systems, the input of chemistry, physics and mathematics is fundamental for the development of an integrative view of life phenomena.

In the quantitative description of the growth of a population, several interactions are involved. There are intrinsic interactions between each organism and its environment and biotic interactions between individuals of the same or of different species. These interactions have specific characteristic times or time scales, and affect the growth and fate of a species or a community of species. Population dynamics deals with the population growth within a short time scale, where evolutionary changes and mutations do not affect significantly the growth of the population, and the population is physiologically stable. In this short time scale, the variation of the number of individuals in the population is determined by reproduction and death rates, food supply, climate changes and biotic interactions, like predation, competition, mutualism, parasitism, disease and social context.

There exists an intrinsic difficulty in analysing the factors influencing the growth and death of a species. There are species that are in the middle of a trophic web, being simultaneously preys and predators, and the trophic web exhibits a large number of interactions. For example, the food web of Little Rock Lake, Wisconsin, shows thousands of inter-specific connections between the top levels predators down to the phytoplankton, [1]. In this context, organisms in batch cultures and the human population are the simplest populations. In batch cultures, organisms interact with their resources for reproduction and growth. The human population is at the top of a trophic chain. Even for each of these simple cases, we can have different modelling approaches and strategies.

From the observational point of view, one of the best-known populations is the human population for which we have more than 50 years of relatively accurate census, and some estimates of population numbers over larger time intervals. Observations of population growth of micro-organisms in batch cultures are important to validate models and to test growth projections based on mathematical models.

Mathematical models give an important contribution to ecological studies. They

propose quantities that can be measured, define concepts enabling to quantify biological interactions, and even propose different modelling strategies with different assumptions to describe particular features of the populations.

In population dynamics, and from the mathematical point of view, there are essentially two major modelling strategies: i) The continuous time approach using techniques of ordinary differential equations; ii) The discrete time approach which is more closely related with the structure of the census of a population. Both approaches use extensively techniques of the qualitative theory of dynamical systems.

In the continuous time approach, the number of individuals of a population varies continuously in time and the most common modelling framework applies to the description of the types of biotic inter-specific interactions and to the interactions of one species with the environment. They are useful for the determination of the fate of a single population or of a small number of interacting species. These models have been pioneered by Pierre-Françoise Verhulst, in the 19th century, with the introduction of the logistic model, and by Vito Volterra, in the first quarter of the 20th century, with the introduction of a model to describe qualitatively the cycling behaviour of communities of carnivore and herbivore fishes.

In the discrete time approach, models are built in order to describe the census data of populations. They are discontinuous in time, and are closer to the way population growth data are obtained. These models are useful for short time prediction, and their parameters can be easily estimated from census data.

Modern ecology relies strongly on the concepts of carrying capacity (of the environment) and growth rate of a population, introduced by the discrete and the continuous models. In the 20th century, the works of McKendrick and Leslie gave an important contribution to modern ecology and demography.

The usefulness of population dynamics to predictability and resource management depends on the underlying assumptions of the theoretical models. Our goal here is to introduce in a single text the most common quantitative approaches to population dynamics, emphasizing the different theoretical foundations and assumptions.

In the next two sections, we introduce the continuous and the discrete age-structured approach to quantitative ecology. These are essentially two review sections, where we emphasise on the assumptions made in the derivation of the models, and whenever possible, we present case studies taken from real data. As the reader has not necessarily a background on the techniques of the qualitative theory of dynamical systems, we introduce some of its geometric tools and the concept of structural stability. In modelling situations where there exists some arbitrariness, structural stability is a useful tool to infer about the qualitative aspects of the solutions of ordinary differential equations upon small variations of its functional forms.

In section 4, and in the sequence of the Leslie type age-structured discrete models (Sec. 3), we make the mathematical analysis of the Portuguese population based

on the census data for the second half of the 20th century. Here we introduce a very simple model in order to interpret data and make demographic projections, to analyse migrations and the change of socio-economic factors. This is a very simple example that shows the importance of mathematical modelling and analysis in population studies. In section 5 we introduce discrete time models with population dependent growth rates, and we analyse the phenomenon of chaos. In section 6, the consumer-resources interaction is introduced, and we discuss the two types of randomness found in dynamical systems: quasi-periodicity and chaos. In section 7, we derive a general approach to the study of population dispersal (short- and long-range), and we derive a simple integro-difference equation to analyse the dispersion of a population.

In section 8, we introduce the standard continuous model for age-structured density dependent populations, the McKendrick model, showing the existence of time periodic solutions by elementary techniques. In this context, we discuss demography cycles and the concept of growth rate. In section 9, we derive a modified McKendrick model for populations with mitotic type reproduction, and compare the growth rates between populations with sexual and mitotic reproduction types. In the final section, we resume the main conclusions derived along the text and we compare the different properties of the analysed models.

2. Biotic Interactions

2.1. *One species interaction with the environment*

We consider a population of a single species in a territory with a well-defined boundary. Let $x(t)$ be the number of individuals at some time t. The growth rate of the population (by individual) is,

$$\frac{1}{x}\frac{dx}{dt} = r \tag{1}$$

If the growth rate r is a constant, independently of the number of individuals of the population, then equation (1) has the exponential solution $x(t) = x(t_0)e^{r(t-t_0)}$, where $x(t_0)$ is the number of individuals in the population at time t_0. If, $r > 0$, $x(t) \to \infty$, as $t \to \infty$. In a realistic situation, such a population will exhaust resources and will die out in finite time.

Equation (1) with r constant is the Malthusian law of population growth. Exponential growth is in general observed in batch cultures of micro-organisms with a large amount of available resources and fast reproduction times, [2] and [3]. From the solution of equation (1) follows that the doubling time of the initial population (t_d) is related with the growth rate by $t_d = \ln 2/r$. For example, with the data of the world population, [4], we can determine the variation of the doubling time or the growth rate of the human population along historical times, Fig. 1. The curve in Fig. 1 suggests that, for human populations and at a large time scale, the growth rate r cannot be taken constant as in the Malthusian growth law (1), but must depend on other factors, as, for example, large-scale diseases, migrations, *etc.*.

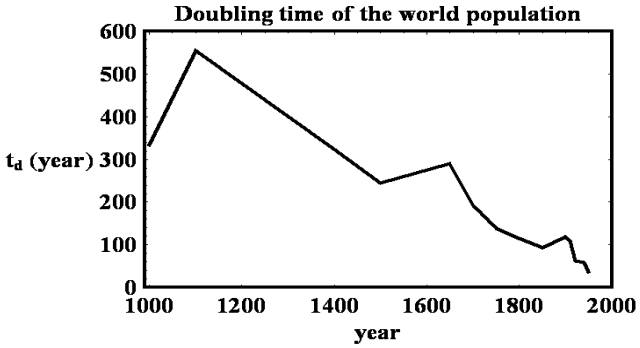

Fig. 1. Evolution of the doubling time of the world population. The doubling time has been calculated according to the formula $t_d = \ln 2/r$, where $r = (N(t+h) - N(t))/(hN(t))$, and $N(t)$ is the world population at year t. The data set is from reference [4].

For large population densities, and in order to avoid unrealistic situations of exponential growth or explosion of population numbers, it is expected that the growth rate becomes population dependent. Assuming that, for large population numbers, $r \equiv r(x(t)) < 0$, for $x > K$, and, $r \equiv r(x(t)) > 0$, for $x < K$, where K is some arbitrary constant, the simplest form for the growth rate $r(x)$ is, $r(x) = r_0(K - x)$. Substitution of this population dependent growth rate into equation (1) gives,

$$\frac{dx}{dt} = r_0 x(K - x) := rx(1 - x/K) \tag{2}$$

where r_0 is a rate constant. Equation (2) is the logistic or Verhulst equation for one-species populations. For a population with $x(t_0) > 0$ at some time t_0, the general solution of (2) is,

$$x(t) = \frac{x(t_0)Ke^{r_0(t-t_0)}}{x(t_0)(e^{r_0(t-t_0)} - 1) + K} \tag{3}$$

and, in the limit $t \to \infty$, $x(t) \to K$. The constant K is called the *carrying capacity* of the environment and is defined as the maximum number of individuals of a species that the territory can support. For the same species, larger territories and bigger renewable resources correspond to larger values of K.

The logistic equation (2) describes qualitatively the growth of single colonies of micro-organisms in batch experiments, [3]. For example, in a batch experiment, Gause, [5], fitted the measured growth curve of the protozoa *Paramecium caudatum*, finding a good agreement with the solution (3) of the logistic equation. For the human population, the agreement is not so good, being dependent on technological developments, sociological trends and other factors, [2]. Depending on the data set, and from country to country, some authors find a good fit between the solutions of the logistic equation and demography data (see for example [4]), and others propose

empirical models based on the delayed logistic equation, $x'(t) = rx^{\alpha}(1-x(t-T)/K)$, [4].

In the derivation of the logistic equation, the plausibility of the mathematical form of the growth rate is assumed, without any assumptions about the relations between population growth and environmental support, or about the mechanisms of interaction between individuals and the environment. It is simply supposed that, for each species, the environment ensures enough resources. The carrying capacity constant can only be measured *a posteriori* through the asymptotic solution, $x(t) \to K$, as $t \to \infty$.

A possible mechanism for the derivation of the logistic equation is based on the mass action law of chemical kinetics, [6] and [7, p. 295-300]. To be more specific, we represent species and resources by, A_j, with $j = 1, \ldots, m$. The interactions between species or between species and resources can be represented by n collision diagrams,

$$\nu_{i1}A_1 + \cdots + \nu_{im}A_m \xrightarrow{r_i} \mu_{i1}A_1 + \cdots + \mu_{im}A_m\,, \quad i = 1, \ldots, n \tag{4}$$

where r_i measure the rate at which the interactions occur, and the constants ν_{ij} and μ_{ij} are positive parameters measuring the number of individuals or units of resources that are consumed or produced in a collision. The mass action law asserts that the time evolution of the (mean) concentration of A_j is given by,

$$\frac{dA_j}{dt} = \sum_{i=1}^{n} r_i(\mu_{ij} - \nu_{ij})A_1^{\nu_{i1}} \ldots A_m^{\nu_{im}}\,, \quad j = 1, \ldots, m \tag{5}$$

As we have in general n interaction diagrams and m species or resources, the system of equations (5) are not independent. In general, by simple inspection of the m equations (5), it is possible to derive the associated conservation laws, that is, a set of linear relations between the concentrations A_j. With these conservations laws, we obtain a system of $s \leq m$ linearly independent differential equations.

In this framework, reproduction in the presence of resources can be seen as the collision of the members of a population with the resources. In the case of the logistic equation, the collisions between individuals and the resource is represented by the diagram,

$$A + x \xrightarrow{r_0} (1+e)x \tag{6}$$

where A represents resources, x is the number of individuals in the population, collisions occur at the rate r_0, and the inequality $e > 0$ expresses the increase in the number of individuals. By (4) and (5), to the diagram (6) is associated the logistic equation (2), together with the conservation law $x(t) + eA(t) = x(t_0) + eA(t_0)$, where the carrying capacity is given by $K = x(t_0) + eA(t_0)$. As, in the limit $t \to \infty$, $x(t) \to K$, then, in the same limit, $A(t) \to 0$. In this interpretative framework, when the population attains the equilibrium value K, resources are exhausted. In realistic situations, after reaching the equilibrium, the number of individuals of the population decreases and, some time afterwards, the population disappears, [3]. However, this asymptotic behaviour is not predicted by equation (2). To further

include this effect, we can add to the collision mechanism (6) a new death rate diagram, $x \xrightarrow{d}$. In this case, by the mass action law, (4) and (5), the time variation of the number of individuals of the population is not of logistic type anymore, obeying to the equations,

$$\begin{cases} x'(t) = r_0 exA - dx \\ A'(t) = -r_0 xA \end{cases} \tag{7}$$

without any conservation law and, consequently, without a carrying capacity parameter. Numerical integration of the system of equations (7) leads to the conclusion that, for a small initial population, a fast exponential growing phase is followed by a decrease in the number of individuals of the population, and extinction occurs when $t \to \infty$, Fig. 2a). The growth behaviour predicted by equation (7) is in qualitative agreement with the growth curves observed in generic microbiological batch experiments, [3].

In Fig. 2a), we compare the solutions of the three equations (1), (2) and (7) for the growth of one-species. In the growing phase, the solutions of the three growth models show qualitatively the same type of exponential behaviour. For equation (7), the concept of carrying capacity is lost but the growth maximum is approximated by the value of the carrying capacity of the logistic equation. In these models, and for the same data set, it is possible to obtain different values for the fitted growth rates, as it is clearly seen in Fig. 2b).

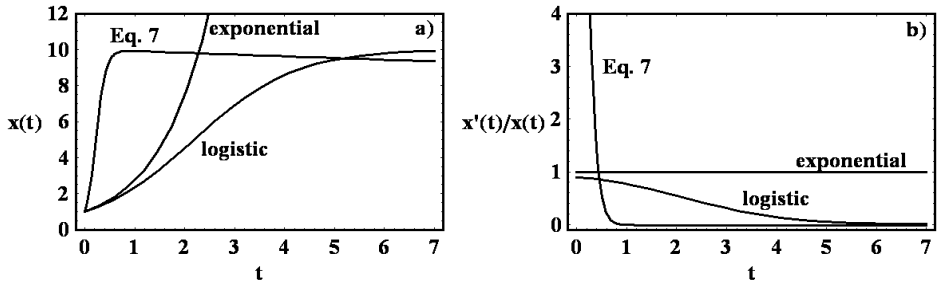

Fig. 2. a) Comparison between the solutions of the exponential (1), logistic (2) and equation (7), for the initial conditions $x(0) = 1$, $A(0) = 9$, and the parameters $r = 1$, $r_0 = 1$, $K = 10$, $d = 0.01$ and $e = 1$. b) Growth rates as a function of time for equations (1), (2) and (7).

The approach developed so far introduces into the language of population dynamics the concepts of exponential or Malthusian growth, growth rate, doubling time and carrying capacity. The agreement between the models and data from laboratory experiments is, in some situations, very good, but in others deviates from observations. In the situations where no agreement with observations is found, it is believed that other relevant factors besides reproduction are not included in the modelling process. In modern ecology, the modelling concepts introduced here en-

able a rough estimate of the population growth and are the starting point for more specific and specialized approaches. For a more extensive study and applications of the exponential and logistic models see [8], [9] and [10].

2.2. *Two interacting species*

Here, we introduce the basic models for the different types of biotic interactions between the populations of two different species. As models become non-linear, and no general methods for the determination of solutions of non-linear differential equations exist, in parallel, we introduce some of the techniques of the qualitative theory of differential equations (dynamical systems theory).

We consider two interacting species in the same territory, and we denote by $x(t)$ and $y(t)$, their total population numbers at time t. The growth rates by individual of both interacting species are,

$$\begin{cases} \frac{1}{x}\frac{dx}{dt} = f(x,y) \\ \frac{1}{y}\frac{dy}{dt} = g(x,y) \end{cases}$$

defining the two-dimensional system of differential equations, or vector field,

$$\begin{cases} \frac{dx}{dt} = xf(x,y) \\ \frac{dy}{dt} = y\,g(x,y) \end{cases} \tag{8}$$

The particular form of the system of equations (8) ensures that the coordinate axes of the (x,y) phase space are invariant for the flow defined by the vector field (8), in the sense that, any initial condition within any one of the coordinate axis is transported by the phase flow along that axis. Due to this particular invariant property, in the literature of ecology, equations (8) are said to have the Kolmogoroff form, [8, p. 62].

In general, the system of differential equations (8) is non-linear and there are no general methods to integrate it explicitly. We can overcome this problem by looking at equation (8) as defining a flow or vector field in the first quadrant of the two-dimensional phase space ($x \geq 0, y \geq 0$). Adopting this point of view, the flow lines are the images of the solutions of the differential equation in the phase space, Fig. 3. At each point in phase space, the flow lines have a tangent vector whose coordinates are $xf(x,y)$ and $yg(x,y)$, and the flow lines can be visualised through the graph of the vector field. In fact, given a set of points in phase space, we can calculate the x- and y-coordinates of the vector field components, $xf(x,y)$ and $yg(x,y)$, and draw the directions of the tangent vectors to the flow lines. The solutions of the differential equation (8) are tangent to the vector field.

The phase space points for which we have simultaneously, $xf(x,y) = 0$ and $yg(x,y) = 0$, are the fixed points of the flow. The fixed points are stationary solutions of the ordinary differential equation (8). In dimension two, the knowledge of these stationary solutions determines the overall topology of the flow lines in

phase space. With the additional knowledge of the two nullclines, defined by equations $xf(x,y) = 0$ and $yg(x,y) = 0$, we can qualitatively draw in phase space the flow lines of the differential equation and to determine the asymptotic states of the dynamics, which, in generic cases, are isolated fixed points.

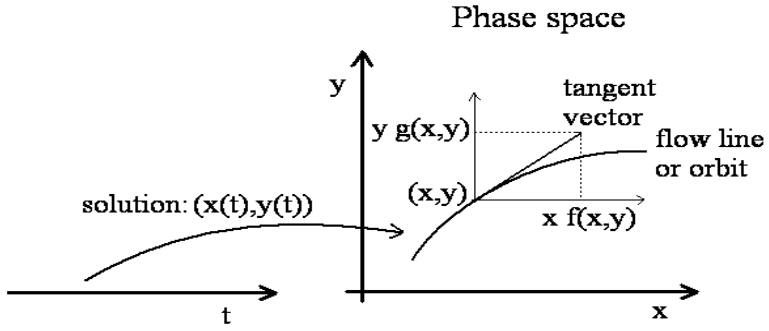

Fig. 3. The differential equation (8) defines a vector field or phase flow in the two-dimensional phase space. The flow lines are the images in phase space of the solutions of the differential equation. The flow lines are parameterised by the time t. At each point (x, y) in phase space, the tangent vector to the flow line or orbit has local coordinates $xf(x,y)$ and $yg(x,y)$.

The (isolated) fixed points of a differential equation can be (Lyapunov-) stable or unstable. They are stable if, for any initial condition close to the fixed point, and for each $t > 0$, the solution of the equation remain at a finite distance from the fixed point. If in addition, in the limit $t \to \infty$, the solution converges to the fixed point, we say that the fixed point is asymptotically stable. A fixed point is unstable if it is not stable.

Around a fixed point, the stability properties of the solutions of a differential equation can be easily analysed. Let (x^*, y^*) be a fixed point of equation (8), and let $(x(t) = x^* + \bar{x}(t),\ y(t) = y^* + \bar{y}(t))$ be a solution defined locally around (x^*, y^*). Introducing this solution into (8), we obtain, up to the first order in $\bar{x}$ and $\bar{y}$,

$$\begin{pmatrix} \frac{d\overline{x}}{dt} \\ \frac{d\overline{y}}{dt} \end{pmatrix} = \begin{pmatrix} f(x^*,y^*) + x^*\frac{\partial f}{\partial x}(x^*,y^*) & x^*\frac{\partial f}{\partial y}(x^*,y^*) \\ y^*\frac{\partial g}{\partial x}(x^*,y^*) & g(x^*,y^*) + y^*\frac{\partial g}{\partial y}(x^*,y^*) \end{pmatrix} \begin{pmatrix} \overline{x} \\ \overline{y} \end{pmatrix} =: DF \begin{pmatrix} \overline{x} \\ \overline{y} \end{pmatrix} \tag{9}$$

where DF is the Jacobian matrix of the vector field (8) evaluated at (x^*, y^*). In the conditions of the theorem below, the solutions of the linear differential equation (9) are equivalent to the solutions of the nonlinear equation (8) near (x^*, y^*).

Theorem 1: (Hartman-Grobman, [11]) If none of the eigenvalues of the Jacobian matrix DF rest on the imaginary axis of the complex plane, then, near the fixed point (x^*, y^*), the phase flows of equations (8) and (9) are similar or topologically equivalent.

Under the conditions of the Hartman-Grobman theorem (Theorem 1), by a simple linear analysis, it is possible to determine the stability of the fixed points of the non-linear equation (8), and, therefore, to determine the asymptotic behaviour of the solutions of the non-linear equation (8). The global flow in the first quadrant of phase space is conditioned by the fixed points with non-negative coordinates. This approach is geometrically intuitive and is one of the most powerful tools of the theory of dynamical systems, [11] and [12]. As will see now, this enables the analysis of models for biotic interactions with a minimum of technicalities.

We now introduce the most common types of two-species interactions. There are essentially three basic two-species interactions: prey-predator, competition and mutualism. In the prey-predator interaction, for large predator numbers, the growth rate of the prey becomes negative, but in the absence of predators, the growth rate of the prey is positive. If the prey is not the only resource for predators, the growth rate of the predators is always positive. In competition, and in the presence of both species, both growth rates decrease. In mutualistic interactions, the growth rates of both species increase.

Adopting the same empirical formalism as in the case of the logistic equation (Sec. 2.1), we assume that the growth rates f and g are sufficiently well behaved functions, and the above ecology definitions can be stated into the mathematical form:

$$\begin{array}{ll} \text{Prey-predator:} & \dfrac{\partial f}{\partial y} < 0, \dfrac{\partial g}{\partial x} > 0 \\ \text{Competition:} & \dfrac{\partial f}{\partial y} < 0, \dfrac{\partial g}{\partial x} < 0 \\ \text{Mutualism :} & \dfrac{\partial f}{\partial y} > 0, \dfrac{\partial g}{\partial x} > 0 \end{array} \tag{10}$$

In the simplest situation where f and g are affine functions, $f(x,y) = d_1 + d_2 x + d_3 y$ and $g(x,y) = d_4 + d_5 x + d_6 y$, and further assuming that in the absence of one of the species the growth of the other species is of logistic type, by (10), we obtain for the growth rates,

$$\begin{array}{lll} \text{Prey-predator:} & f = r_x(1 - x/K_x - c_1 y) \text{ and } & g = r_y(1 + c_2 x - y/K_y) \\ \text{Competition:} & f = r_x(1 - x/K_x - c_1 y) \text{ and } & g = r_y(1 - c_2 x - y/K_y) \\ \text{Mutualism:} & f = r_x(1 - x/K_x + c_1 y) \text{ and } & g = r_y(1 + c_2 x - y/K_y) \end{array} \tag{11}$$

where c_1, c_2, K_x and K_y are positive constants. The constants in the growth rate functional forms (11) have been chosen in such a way that, in the absence of any one of the species, we obtain the logistic equation (2). Introducing (11) into (8), we obtain three systems of non-linear ordinary differential equations for prey-predation, competition and mutualism. The topological structure in phase space of the solutions of these equations can be easily analysed by the qualitative methods just described above.

The generic differential equation (8) defines a flow in the first quadrant of the two-dimensional phase space, and the simplest solutions are the fixed points of the flow. These fixed points are obtained by solving simultaneously the equations,

$xf(x,y) = 0$ and $yg(x,y) = 0$. For any of the values of the parameters in (11), and for the three biotic interaction types, we have the fixed points $(x_0, y_0) = (0, 0)$, $(x_1, y_1) = (K_x, 0)$ and $(x_2, y_2) = (0, K_y)$, which correspond to the absence of one or both species. The fixed points $(K_x, 0)$ and $(0, K_y)$ are the asymptotic solutions associated to any non-zero initial condition on the phase space axis x and y, respectively. The zero fixed point corresponds to the absence of both species. For a particular choice of the parameters, a forth fixed point can exists:

$$\begin{array}{ll}
\text{Prey-predator:} & (x_3, y_3) = (K_x \frac{1-c_1K_y}{1+c_1c_2K_xK_y}, K_y \frac{1+c_2K_x}{1+c_1c_2K_xK_y}) \text{ if } c_1K_y < 1 \\
\text{Competition:} & (x_3, y_3) = (K_x \frac{c_1K_y-1}{c_1c_2K_xK_y-1}, K_y \frac{c_2K_x-1}{c_1c_2K_xK_y-1}) \text{ if } c_1K_y > 1,\ c_2K_x > 1 \\
\text{Mutualism:} & (x_3, y_3) = (K_x \frac{1+c_1K_y}{1-c_1c_2K_xK_y}, K_y \frac{1+c_2K_x}{1-c_1c_2K_xK_y}) \text{ if } c_1c_2K_xK_y < 1
\end{array} \tag{12}$$

In Fig. 4, we show, for the differential equation (8) and the three growth rate functions (11), all the qualitative structures of the flows in phase space. The fixed points with non-zero coordinates (12) correspond to cases a)-c), and are marked with a square.

To determine qualitatively the structure of the solutions of equation (8) for the different cases depicted in Fig. 4, we have analysed the signs of the components of the vector field along the nullclines. The arrows in Fig. 4 represent the directions of the flow in phase space. Except the case of Fig. 4a), the vector field directs the flow towards the fixed points, and the limiting behaviour of the solutions as $t \to \infty$ is easily derived.

To analyse the prey-predator case of Fig. 4a), we have calculated the directions of the vector field near the fixed point (x_3, y_3), Fig. 5. In this case, the flow turns around the fixed point (x_3, y_3), and to determine the local structure of the flow, we use the technique provided by the Hartman-Grobman theorem. Linearising equation (8) around (x_3, y_3), by (11) and (12), we obtain the linear system of differential equations,

$$\begin{pmatrix} \frac{d\overline{x}}{dt} \\ \frac{d\overline{y}}{dt} \end{pmatrix} = \begin{pmatrix} -r_x x_3/K_x & -r_x x_3 c_1 K_x \\ r_y c_2 y_3 & -r_y y_3/K_y \end{pmatrix} \begin{pmatrix} \overline{x} \\ \overline{y} \end{pmatrix} = DF \begin{pmatrix} \overline{x} \\ \overline{y} \end{pmatrix} \tag{13}$$

where $(x, y) = (x_3 + \overline{x}, y_3 + \overline{y})$. The stability near the fixed point (x_3, y_3) is determined by the eigenvalues of the matrix DF, provided that they are not on the imaginary axis of the complex plane. As, $Trace(DF) = \lambda_1 + \lambda_2 < 0$ and $Det(DF) = \lambda_1\lambda_2 > 0$, the eigenvalues λ_1 and λ_2 of DF are both real and negative or, complex conjugate with negative real parts. As the solution of the linear system of equations (13) is a linear combination of terms of the form $e^{\lambda_i t}$, and the eigenvalues have negative real parts, this implies that $\overline{x}(t)$ and $\overline{y}(t)$ converge to zero as $t \to \infty$. Therefore, for non-zero initial conditions, the solutions of the prey-predator system of Fig. 4a) converge to the stable fixed point (x_3, y_3), Fig. 5.

In the prey-predator case of Fig. 4d), $c_1K_y > 1$, the effect of the predator on the prey is so strong that asymptotically predators consume all the preys, and, as

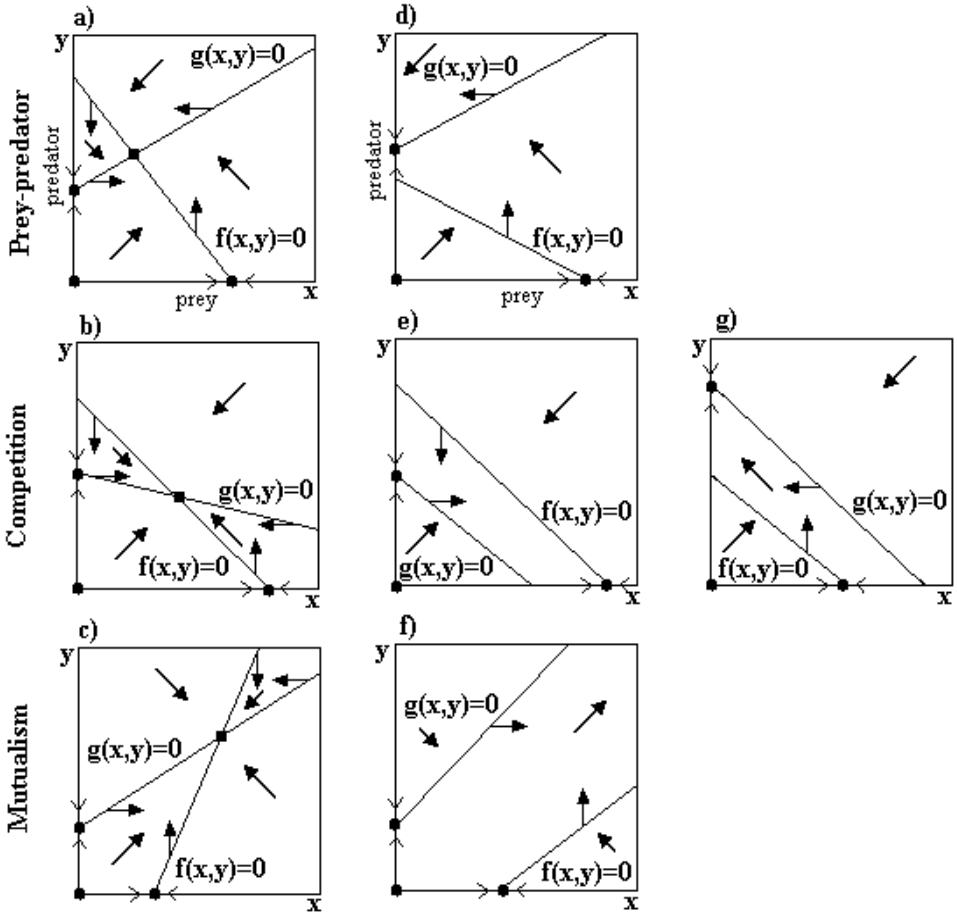

Fig. 4. Qualitative structures of the flow in phase space of the differential equation (8), for the growth rate functions (11). Bullets and squares represent fixed points. In cases a)-c), a non-zero fixed point exists if the conditions in (12) are verified. Cases d)-g) correspond to different arrangements of nullclines. The arrows represent the directions of the vector fields, and the solutions of equation (8) are tangent to the vector field. The sign of the vector field is calculated from the sign of the functions f and g at each point in phase space.

$t \to \infty$, the solutions converge for the fixed point $(x_2, y_2) = (0, K_y)$. In this case, we do not need to make the linear analysis near the fixed points because the directions of the vector field show clearly the convergence of the solutions to the asymptotically stable fixed point.

For the competitive and mutualistic interactions of Figs. 4b) and 4c), equation (8) has always a stable fixed point which is also an asymptotic solution for non-zero initial conditions. In cases e) and g), we have $c_1 K_y < 1$ or $c_2 K_x < 1$, and, asymptotically in time, only one of the species survives. For the mutualistic interaction f), we

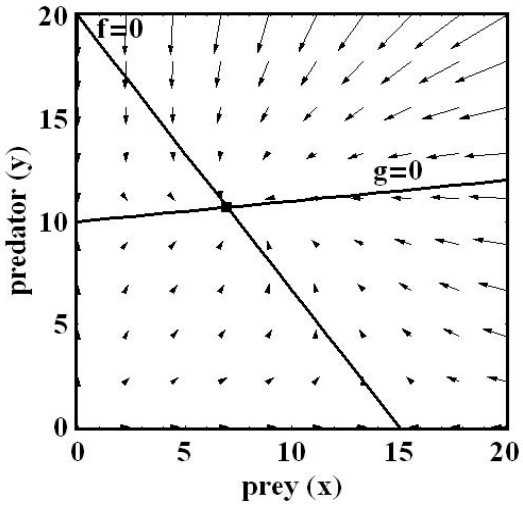

Fig. 5. Vector field and nullclines for the prey-predator equation of Fig. 4a), with parameter values $c_1 = 0.05$, $c_2 = 0.01$, $K_x = 15$, $K_y = 10$ and $r_x = r_y = 1$. As it is clearly seen, the vector field directs the flow to the fixed point (x_3, y_3). This fixed point is asymptotically stable.

have $c_1 c_2 K_x K_y > 1$, and, asymptotically in time, both population numbers explode to infinity. (Note however that, in this last case, it is possible that the solutions go to infinity in finite time due to the non-Lipschitz nature of the right hand side of (8).)

From the models for the prey-predator, competition and mutualistic interactions, it is possible to derive some ecological consequences. In the prey-predator system, the prey brings advantage to the predator in the sense that its presence increases the number of predators at equilibrium, but the presence of predator decreases the equilibrium population of the prey. If the effect of the predator on the prey is too strong, predators consume all the preys, and, in the long time scale, predators lose advantage.

For competition, the asymptotic equilibrium between the two species assumes lower values for both species when compared to the cases where they are isolated.

In the mutualistic interaction, the situation is opposed to the competition case, where the equilibrium between the two species assumes higher values. However, for strong mutualistic interactions, we can have overcrowding as in the Malthusian model (1), leading to the death of the species by over consumption of resources. These conclusions, derived from the mathematical models (8) and (11), are in agreement with the biological knowledge about predation, competition and mutualism, [13] and [14].

Another model for the prey-predator interaction that has a conceptual and historical importance is the Lotka-Volterra model. This model has been used as an explanation to justify the resumption of carnivore fishes, after the cessation of fish-

ing in the North Adriatic Sea after the First World War, [8]. To be more specific, the prey-predator Lotka-Volterra interaction model is,

$$\begin{cases} \frac{dx}{dt} = r_x x(1 - c_1 y) \\ \frac{dy}{dt} = r_y y(c_2 x - 1) \end{cases} \tag{14}$$

where c_1, c_2, r_x and r_y are constants.

This model obeys the prey-predator conditions in (10), but assumes that predators have an intrinsic negative growth rate and do not survive without preys. For preys alone, it assumes that they have exponential growth as in model (1).

The Lotka-Voltrerra model (14) has one horizontal and one vertical nullcline in phase space, Fig. 6, and one non-zero fixed point with coordinates $(x, y) = (1/c_2, 1/c_1)$. One of the eigenvalues of the Jacobian matrix of (14) calculated at the fixed point is zero, and as the conditions on the Hartman-Grobman theorem fail: the local structure of the flow cannot be characterized by the linear analysis around the fixed point. It can be shown that, in the first quadrant of phase space, the solution orbits of (14) are closed curves around the fixed point, Fig. 6, corresponding to oscillatory motion in the prey and predator time series (for a proof see [12]). Moreover, along each phase space cycle, the temporal means of prey and predators are independent of the amplitude of the cycles, being given by, $\langle x \rangle = 1/c_2$ and $\langle y \rangle = 1/c_1$, respectively. This property of the solutions of equations (14) has been used to assert that fluctuations in fisheries are periodic but the time average during each cycle is conserved, [8, p. 93].

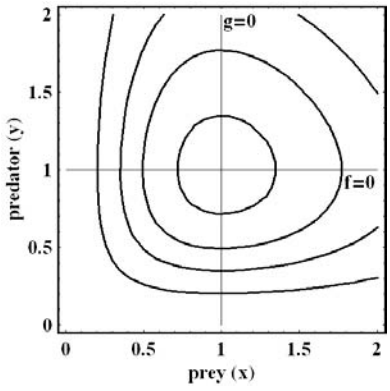

Fig. 6. Qualitative structure of the flow in phase space of the Lotka-Volterra system of equations (14), for parameter values $c_1 = c_2 = r_x = r_y = 1$. Away from the non-zero fixed point, the solutions are periodic in time, suggesting a simple explanation for the oscillatory behaviour observed in prey-predator real systems. It can be shown that the orbits of the system of equations (14) are the level sets of the function, $H(x, y) = r_y \log x - r_y c_2 x + r_x \log y - r_x c_1 y$.

One of the important issues in the Lotka-Volterra model is to suggest the possibility of existence of time oscillations in prey-predator systems. A long-term ob-

servation of prey-predator oscillations was provided by the hare-lynx catches data during 90 years, from the Hudson Bay Company, [14] and [15]. The catches of lynx and hare are in principle proportional to the abundances of these animals in nature, and the time series shows an out of phase oscillatory abundance, with the lynx maximum preceding the hare maximum. Making a naïf analogy between the solutions of the Lotka-Volterra model and the oscillations found in the lynx-hare interaction, it turns out that the maximum number of preys is observed before the maximum numbers of predator. This is in clear disagreement with the Lotka-Volterra model where the prey maximum precedes in time the predator maximum, Fig. 6. Several attempts were made to explain this out of phase behaviour but no consistent explanations have been found, [15].

One possible meaningful argument against the plausibility of the Lotka-Volterra model (14) to describe the prey-predator interaction is based on the property that any perturbation of the right hand side of equation (14) destroys the periodic orbits in phase space. In mathematical terms, it means that the Lotka-Volterra system (14) is not structurally stable or robust. In general, a two-dimensional dynamical system is structurally stable if all its fixed points obey the conditions of the Hartman-Grobman theorem, and there are no phase space orbits connecting unstable fixed points (saddle points), [11] and [12]. The only types of structurally stable two-dimensional differential equations with periodic orbit in phase space are equations with isolated periodic orbits or limit cycles. In this case, the growth rate functions f and g must be at most quadratic, and several models with this property appeared in the literature, [12] and [15]. However, all these models show the same wrong out of phase effect as in the hare-lynx data.

In modern theoretical ecology, the development of more specialized models relies on the conditions (10) and on further assumptions on the functional behaviour of the growth rate functions, [13], [12] and [14]. In some cases, the assumptions are introduced in analogy with some mechanisms derived from chemical kinetics, [6], [16] and [17]. For example, the mechanisms,

$$\begin{aligned} &A + x \xrightarrow{r_1} (1+e_1)x \\ &x + y \xrightarrow{r_2} (1+e_2)y + cx \\ &x \xrightarrow{d_1} \\ &y \xrightarrow{d_2} \end{aligned} \tag{15}$$

with $e_1 > 0$, $e_2 > 0$, $r_1 > 0$, $r_2 > 0$ and $c < 1$, and,

$$\begin{aligned} &A + x \xrightarrow{r_1} (1+e_1)x \\ &B + y \xrightarrow{r_2} (1+e_2)y \\ &x + y \xrightarrow{r_3} c_1 x + c_2 y \\ &x \xrightarrow{d_1} \\ &y \xrightarrow{d_2} \end{aligned} \tag{16}$$

with $e_1 > 0$, $e_2 > 0$, $r_1 > 0$, $r_2 > 0$, $r_3 > 0$, $c_1 > 0$ and $c_2 > 0$, are examples

of possible mechanisms for the prey-predator and generic biotic interactions. The phase space structure of the orbits of the Lotka-Volterra system (14) and the model (8)-(11) are different from the ones derived from the model equations associated to (15) and (16). However, the mechanistic interpretation of models (15) and (16) are closer to the biological situations. A detailed account of models for predation and parasitism is analysed in [18] and [19].

3. Discrete models for single populations. Age-structured models

One important fact about the individuals of a species is the existence of age classes and life stages. Within each age class, the individuals of a species behave differently, have different types of dependencies on the environment, have different resource needs, *etc.*. For example, in insets, three stages are generally identified: egg, larval and the adult. In mammals, in the childhood phase, reproduction is not possible, neither hunting nor predation.

To describe a population with age classes or stages, we can adopt a discrete formalism, where the transition between different age classes or stages is described in matrix form. One of the advantages of this type of models is that they can be naturally related with field data. One discrete model that accounts for age or stage classes has been proposed by Leslie in 1945, [20].

The Leslie model considers that, at time n, a population is described by a vector of population numbers, $(N^n)^T = (N_1^n, ..., N_m^n)$, where N_i^n is the number of individuals with age class i (or in life stage i). The time transition between age classes is described by the map,

$$N^{n+1} = AN^n \tag{17}$$

where A is the Leslie time transition matrix. Under the hypothesis that from time n to time $n+1$, the individuals die out or change between consecutive age classes, the matrix A has the form,

$$A = \begin{pmatrix} 0 & e_2 & e_3 & \cdots & e_{k-1} & e_k \\ \alpha_1 & 0 & 0 & \cdots & 0 & 0 \\ 0 & \alpha_2 & 0 & \cdots & 0 & 0 \\ \vdots & \vdots & \vdots & \cdots & \vdots & \vdots \\ 0 & 0 & 0 & \cdots & \alpha_{k-1} & 0 \end{pmatrix} \tag{18}$$

where the e_i are fertility coefficients, and the α_i are the fraction of individuals that survive in the transition from age class $i-1$ to i. Clearly, $e_i \geq 0$ and $0 < \alpha_i \leq 1$. We consider always that $e_k > 0$, where e_k is the last reproductive age class. If $e_k = 0$, the determinant of matrix A is zero. Obviously, we can have populations with age classes such that $e_p = 0$ and $\alpha_p > 0$, for $p > k$. In this case, if $e_k > 0$, the solutions N_p^n, with $p > k$, are determined from the solutions obtained from the discrete difference equation (17) in dimension k. For example, if $e_{k+1} = 0$, then

$N_{k+1}^n = \alpha_k N_k^{n-1}$. Therefore, without loss of generality, we always consider that $e_k > 0$ and $e_p = 0$, for $p > k$.

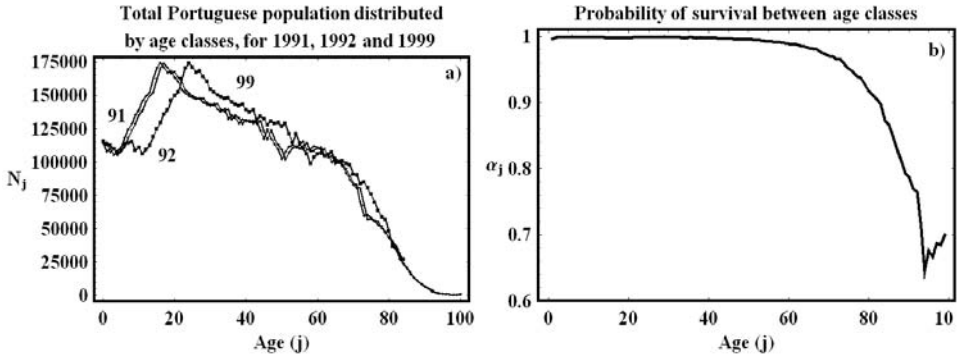

Fig. 7. a) Total Portuguese population distributed by age classes for 1991, 1992 and 1999, [21]. b) Probability of survival between age classes calculated with the population data of 1991 and 1992. The fraction of individuals that survive in the transition from age class $j-1$ to j is given by, $\alpha_j = N_{j+1}^{n+1}/N_j^n$.

In Fig. 7a), we show the distribution of age classes for the Portuguese population obtained from the census of 1991, 1992 and 1999, [21]. As it is clearly seen, the population in 1992 and 1999 is approximately obtained from the population in 1991 by a translation along the age axis, a property shared by the Leslie transition matrix (18). In Fig. 7b), we show the values of the survival probability α_j as a function of the age classes, calculated from the census of 1991–92. For age classes $j < 45$, the values of α_j are close to 1.

The solution of the Leslie discrete map model (17)–(18) is easily determined. As the discrete equation (17) is linear, its general solution is, [22],

$$N_i^n = \sum\nolimits_{j=1}^{k} c_{ij} \lambda_j^n \tag{19}$$

where the c_{ij} are constants determined by the initial conditions and the coefficients of the matrix A, and the λ_j are the eigenvalues of (18). To simplify, we assume that the eigenvalues of A have multiplicity 1. As A is a non-negative matrix with non-zero determinant ($e_k > 0$), by the Frobenius-Perron theory, [23], its dominant eigenvalue λ is positive with multiplicity 1, implying the existence of a non-zero steady state if, and only if, $\lambda = 1$. If, $\lambda < 1$, the solutions (19) go to zero, as $n \to \infty$. If, $\lambda > 1$, the solutions (19) go to infinity.

Calculating the characteristic polynomial of A, we obtain (by induction in k),

$$P(\lambda) = (-1)^k \left(\lambda^k - \sum_{i=2}^{k} e_i \lambda^{k-i} \prod_{j=2}^{i} \alpha_{j-1} \right) \tag{20}$$

Imposing the condition that $\lambda = 1$ is a root of the polynomial (20), from the condition $P(1) = 0$, we define the constant,

$$G := \sum_{i=2}^{k} e_i \prod_{j=2}^{i} \alpha_{j-1} \tag{21}$$

where G is the *inherent net reproductive number of the population*. If we make the approximation, $\alpha_j \approx 1$, we have the *net fertility number* $\overline{G} := \sum_{i=2}^{k} e_i$.

The condition for the existence of asymptotic stable population numbers, given by the dominant eigenvalue of A, can be stated through the inherent net reproductive number of the population. So, in a population where $G < 1$, any initial condition leads to extinction. If, $G > 1$, we have unbounded growth. If, $G = 1$, in the limit $n \to \infty$, the population attains a stable age distribution.

The Leslie model is important to describe populations where there exists a complete knowledge of the life cycle of the species, including survival probabilities and fertilities by age classes. For example, in the Leslie paper [20], it is described a laboratory observation of the growth of *Rattus norvegicus*. For a period of 30 days, the projected total population number was overestimated with an error of 0.06% of the total population.

For human populations, survival probabilities are easily estimated from census data, Fig. 7. However, data from the fertility coefficients are difficult to estimate due to sex distinction and to the distribution of fertility across age classes. For an exhaustive account about Leslie type models, its modifications, and several case studies we refer to [23], [24] and [13]. For tables of the world population by country and the measured parameters of the Leslie matrix, we refer to [25].

Comparing the discrete and the continuous time approaches, the Leslie population growth model presents exactly the same type of unbounded growth as the exponential model (1). To overcome the exponential type of growth, we can adopt two different points of view. One approach is to introduce a dependence of the growth rates on the population numbers, as it has been done in section 2, in the derivation of the logistic equation from the Malthusian growth equation. Another alternative is to introduce a limitation on the growth rates through the resource consumption of the population. These two types of development of the Leslie model lead to the introduction of the concepts of chaos and randomness and will be developed below.

4. A case study with a simple linear discrete model

Here, we introduce a simplified discrete linear model enabling to make projections about human population growth based on census data. With this simple model, we avoid the difficulty associated with the choice of the fertility coefficients by age classes, a characteristic of the Leslie model.

We characterize a population in a finite territory at time n by a two-dimensional vector $(B^n, N^n)^T$, where B^n represents the age class of new-borns, individuals with less than 1 year, and N^n represents the total number of individuals with one or more years. By analogy with the Leslie approach of the previous section, the time evolution equations are now,

$$\begin{pmatrix} B^{n+1} \\ N^{n+1} \end{pmatrix} = \begin{pmatrix} 0 & e \\ \beta & \alpha \end{pmatrix} \begin{pmatrix} B^n \\ N^n \end{pmatrix} \tag{22}$$

where e is the (mean) fertility coefficient of the population, α is the probability of survival of the total population between consecutive years, and β is the probability of survival of new-borns. In census data, the fertility coefficient is given in number of new-borns per thousand, but here we use the convention that the fertility coefficient is given in number of new-borns by individual.

Following the same approach as in the previous section, the solution of the discrete equation (22) is,

$$\begin{aligned} B^n &= c_1\lambda_1^n + c_2\lambda_2^n \\ N^n &= c_3\lambda_1^n + c_4\lambda_2^n \end{aligned} \tag{23}$$

where λ_1 and λ_2 are the eigenvalues of the matrix defined in (22), and the c_i are constants to be determined from the initial data taken at some initial census time n_0. If the dominant eigenvalue of the matrix in (22) is $\lambda = 1$, in the limit $n \to \infty$, the solution (23) converges to a non-zero constant solution, from any non-zero initial data. As the characteristic polynomial of the matrix in (22) is,

$$P(\lambda) = \lambda^2 - \alpha\lambda - e\beta$$

the condition of existence of a non-zero steady state is,

$$I = \alpha + e\beta = 1 \tag{24}$$

As in (21), we say that $I = \alpha + e\beta$ is the inherent net reproductive number of the population. If, $I > 1$, then $\lambda > 1$, and the solution (23) diverges to infinity as $n \to \infty$. If, $I < 1$, then the solution (23) goes to zero.

In order to calibrate the simple model (22), we take the census data for the Portuguese population in the period 1941–1999, Fig. 8.

As we see from Fig. 8, the total Portuguese population without newborns shows strong variations, sometimes with a negative growth rate. This negative growth rate is due to emigration, decrease of population fertility and other social factors. The data for new-borns also shows negative growth rates. Therefore, the growth behaviour shown in Fig. 8 is influenced by other factors that are necessary to quantify.

The values of the parameters α, β and e, are calculated from the census data and are shown in Fig. 9. The probability of survival of the population is approximately constant with mean $\alpha = 0.9891$, and a standard deviation of the order of 10^{-6}. The coefficient of fertility e and the new-borns survival probability β vary along the

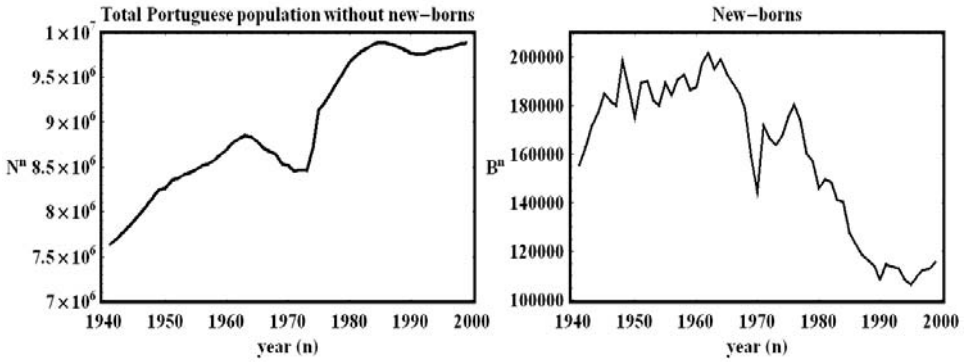

Fig. 8. Portuguese population and new-borns for the years 1941–1999, from reference [21].

years. The last two coefficients are very sensitive to socio-economic and technological factors, suggesting that, for growth predictions, we must introduce into model (22) their time variation.

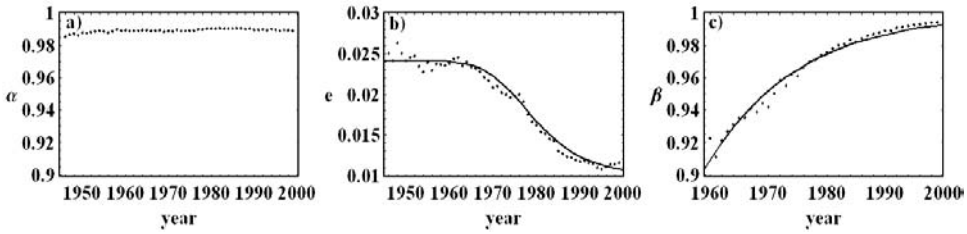

Fig. 9. a) Probability of survival α, and (b) fertility coefficient e for the period 1945–1999. c) Probability of survival of new-borns β in the period 1960–1999. The probabilities of survival α and β have been calculated with the death rate data by thousand habitants, [21]. In b) and c), we show the fitting functions (25), for the parameter values (26).

From the data of Fig. 9, the net reproductive number can be estimated. In Fig. 10, we show the variation of $I = \alpha + e\beta$ for the period 1960–1999. For 1960, we have $I = 1.01137$ and, for 1999, $I = 1.00074$, both very close to the steady state condition (24). Therefore, during this period of time, the Portuguese population is growing with a net reproductive number $I > 1$, but very close to 1. The decrease in the population number in the period 1960-1974 is essentially due to emigration.

To make population growth projections, we consider that α is constant, Fig. 9, with the mean value $\alpha = 0.9891$, and we consider that e and β are time varying functions. Due to the form of the curves in Fig. 9, the functions,

$$\begin{aligned} e(t) &= c_1 + \frac{c_2}{c_3 + (t - 1945)^{c_4}} \\ \beta(t) &= 1 - c_5 e^{-c_6 (t - 1960)} \end{aligned} \tag{25}$$

are reasonable choices, with fitting constants,

$$c_1 = 0.00979232, c_2 = 5.65086 \times 10^6, c_3 = 3.93899 \times 10^8, c_4 = 5.63644$$
$$c_5 = 0.09058, c_6 = 0.06355 \tag{26}$$

In Fig. 9, we show the fitting functions (25), for the parameter values (26). In the limit $t \to \infty$, the new-borns survival probability converges to 1 and the mean fertility coefficient converges to $c_1 \approx 0.0097$, which corresponds roughly to 10 new-borns per thousand individuals in the population. The census value of e for 1999 corresponds to 11.6 new-borns per thousand.

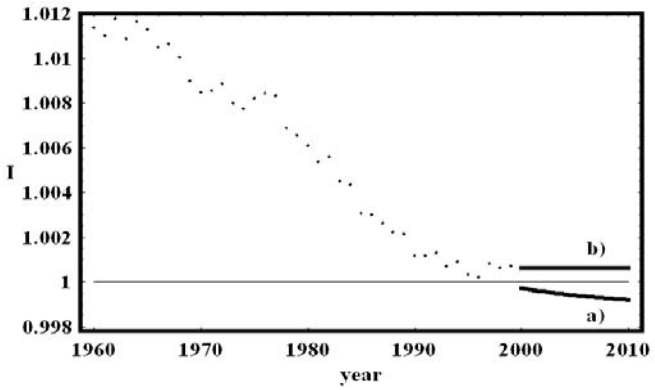

Fig. 10. Dots represent the inherent net reproductive number of the Portuguese population, calculated from the data of Fig. 9 (1960–1999). The two lines correspond to the two possible projections for the net reproductive number I, for the period 2000–2010. In estimate a), we have considered that the time dependence of β and e is given by (25), for the parameter values (26). In estimate b), we have taken constant values for β and e, obtained with the 1999 census values, [21].

To estimate the population growth for the period 2000–2010, we adopt two strategies for the iteration of map (22). In the first case, we iterate (22) with the time dependent functions (25), and we introduce as initial conditions the census data for 1999, Fig. 11. In the second case, we take for β and e the 1999 values. We also apply these two strategies to estimate the net reproductive number (24) as a function of time, Fig. 10.

With the simplified model (22), it is possible to make a short time projection of population numbers. However, for a good calibration and greater accuracy, emigration and immigration factors must be taken into account.

From the data and the fits in Figs. 10 and 11, we can derive several conclusions. The projections for the period 2000–2010 show two different growth behaviours: In case a) of Fig. 10 and 11, we have, $B^{2010} = 99,966$ and $N^{2010} =$ 9,835,840, with $B^{1999} = 115,440$ and $N^{1999} =$ 9,882,150, implying a negative growth with an inherent net reproductive number $I < 1$. In case b), we have, $B^{2010} = 115,251$ and

$N^{2010} = 9{,}940{,}660$, corresponding to a positive growth of the population but with I close to the transition value $I = 1$.

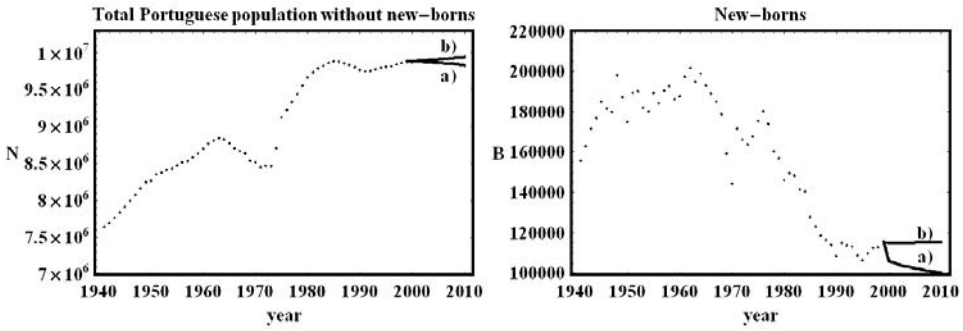

Fig. 11. Projections of the population numbers for the period 2000–2010, from the initial data of the year 1999. In estimate a) we have considered that the time dependence of β and e is given by (25)-(26). In the estimate b), we took β and e with the 1999 census values. These projections do not take into account emigration or immigration factors.

Emigration and immigration are strongly dependent on several social factors. However, even in this simplified model, we can make an estimate of the balance between emigration and immigration. Iterating map (22) for all the initial conditions between 1960 and 1998, we can compare with the census data the projected value for the next year. The differences between these values is an estimate of the balance between emigration and immigration, Fig. 12. In this case, we have used the mean value $\alpha = 0.9891$, which does not change too much during the period under analysis.

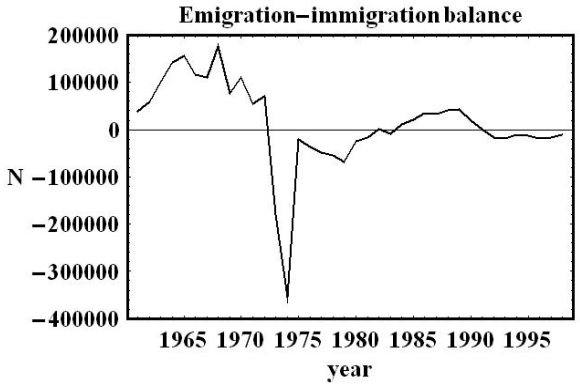

Fig. 12. Emigration-immigration balance for the period 1961-1999 calculated with the census data and model equation (22). Positive values correspond to larger emigration when compared to immigration. Negative values mean that immigration is larger than emigration.

The period 1960–1974 is characterized by a strong emigration, reflected in the negative growth of the population and new-borns. During the period 1974–1982, immigrants outnumber emigrants, introducing a larger growth in the population and in the newborns. For the period 1983–1999, we have an oscillatory balance. In the period 1960–1974, the emigration-immigration balance is of the order of 0.68 millions habitants, implying that emigration was stronger than immigration. In the period 1975–1999, the external income of population dominates, and the emigration-immigration balance is of the order of -0.18 millions habitants.

The example presented here shows how this type of simple discrete models can help us to predict the overall growth of a population, the impact of historical events and the impact of policies of social protection and medical care. In fact, the main features presented in the figures reflect important social transformations that occurred in Portugal in the last 40 years. This approach can be further extended in order to introduce emigration and immigration factors and age classes.

In fact, in demography studies, the Leslie discrete model of section 3 is nowadays the basic tool for demographic projections in human populations, [25]. In microbiology, most of modelling approaches are based on the exponential and logistic models, [3].

5. Discrete time models with population dependent parameters

In discrete time models with population dependent parameters, we introduce the same kind of reasoning as developed in the continuous models of Sec. 2: In a bounded territory, the growth rate of a population shows sensitivity to population numbers, Fig. 1. As we have seen, this choice has been used in the derivation of the logistic model and, in some sense, has been validated by the predictions of growth of *Paramecium caudatum* in a batch culture.

The simplest discrete population dependent model is described by the Ricker map [26],

$$N_{n+1} = rN_n e^{-N_n} \tag{27}$$

where r is the growth rate and N_n represents the number of individuals of a population at time n. This map has been used for many years in the analysis of fisheries.

The overall dynamics of map (27) is similar to the discrete logistic model,

$$N_{n+1} = aN_n(1 - N_n) \tag{28}$$

used in the modern theory of dynamical systems as a prototype of a chaotic systems, [27]. In particular, the map (28) is a finite differences approximation to the logistic equation (2). Applying a finite difference approximation for the derivative in (2), we obtain, $x_{n+1} = x_n(1 + r\Delta t - x_n r\Delta t/K)$. With the linear change of coordinates, $N_n = r\Delta t x_n/K(r\Delta t + 1)$ and $a = (r\Delta t + 1)$, we get the discrete logistic map (28). These types of models introduce a population dependent growth rate in the form of a decreasing function of the number of individuals in the population. The right hand

side of both maps (27) and (28) have a local maximum at $N_n = 1$ and $N_n = 1/2$, respectively.

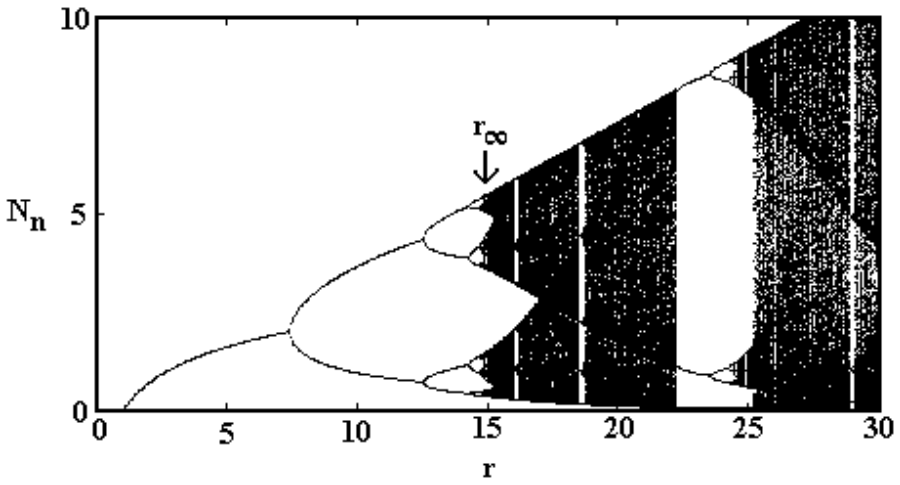

Fig. 13. Bifurcation diagram for the Ricker map (27). Chaos occurs for $r > r_\infty$.

The dynamic behaviour of maps (27) and (28) introduce into the language of population dynamics and ecology the concept of chaos, [27]. The motivation for this approach is based on some observations that, during time, some populations show erratic variations in the population numbers, apparently without external causes, as for example the diminishing of environmental resources.

From the mathematical point of view, there are essentially two types of random behaviour in dynamical systems. One type of random behaviour, called quasi-periodicity, is associated with the non-periodicity of a temporal time series, as in the iteration of circle maps, [11]. The other type of erratic behaviour, called chaoticity, is associated with the existence of an infinite number of unstable periodic orbits in phase space. The Ricker and the logistic maps have chaotic behaviour for several parameter values.

To analyse the type of random behaviour of the Ricker map (27), we construct a bifurcation diagram: For each value of the parameter r, we iterate the Ricker map from a given initial condition, say 1000 times, and we plot the last 500 iterates. Then, we repeat this procedure for other parameter values. The graph obtained gives information about the asymptotic states of the trajectories of the map, as a control parameter is varied, Fig. 13. For simple enough maps, as one-dimensional maps with one maximum, the information obtained by this method is independent of the initial conditions.

As we see from Fig. 13, for small values of the parameter r, the map (27) has

an asymptotically stable steady state — the iterates converge to a stable period-1 fixed point or stable steady state. Increasing the value of the parameter r, the period-1 stable steady state disappears and a new stable steady state with period-2 appears. The parameter value of the transition is a bifurcation in the dynamics of the map. For the parameter values where the period-2 orbit is stable, there exists an unstable period-1 orbit, which obviously does not appear in the bifurcation diagram. For increasing values of the parameter r, a sequence of period doubling bifurcations appears. This sequence accumulates at $r = r_\infty$. For $r > r_\infty$, we say that the dynamics of map (27) is chaotic, [11].

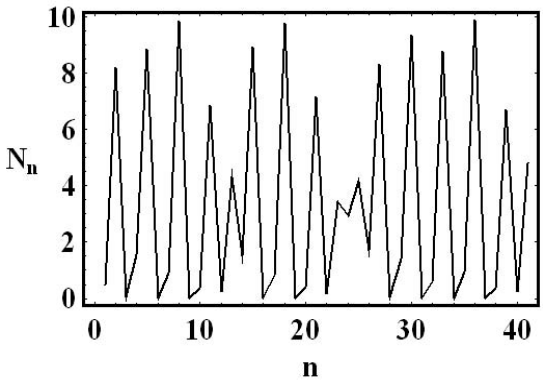

Fig. 14. Chaotic time series obtained with the Ricker map (27), for $r = 26$.

One of the characteristics of the chaotic region in one-dimensional maps ($r > r_\infty$) is the existence of an infinite number of unstable periodic orbits in phase space, even in the regions where the asymptotic states are stable fixed points. The typical time series of a chaotic map is represented in Fig. 14.

It is generally believed that populations can have chaotic behaviour in time [27]. In a laboratory experiment with a flour beetle, Costantino et al. [28] have shown that, by manipulating the adult mortality, the number of individuals of the population can have erratic behaviour in time. In this case, the experimental system shows qualitatively the same type of bifurcation behaviour as in a non-linear three-dimensional discrete model for the time evolution of the feeding larvae, the large larvae and the mature adults. However, there is no clear evidence that such erratic behaviour shares the same dynamic properties of maps with chaotic behaviour, despite the similarities between bifurcation diagrams.

Based on observational data, some authors claim that, in the time series of some populations, the observed erratic behaviour has quasi-periodic characteristics, [29]. In the next section, we present a resource-consumer approach model with a bifurcation diagram with some characteristics that are similar to the one obtained

with the Ricker map.

6. Resource dependent discrete models

The consumer-resource interaction is a fundamental issue in ecology, [30] and [31]: Without resources, living organisms do not survive or reproduce. In a rich environment, it seams natural to assume that the effect of resources on a small population is not an important limiting factor for growth. However, if resources are scarce, we can expect an increase of death rates and an increase in mobility for the search for other territories.

In ecological modelling, the effect of resources is sometimes introduced as external forcing factors. A typical example is the modelling based on the logistic equation with a time varying carrying capacity. In this case, the response of the population numbers to the external forcing follows the time varying characteristics of the forcing function. Here, we adopt a more generic approach and introduce directly the dynamics of the resources into the models, [31].

To maintain some degree of generality in the construction of resource dependent models, we adopt a Leslie age-structured approach. The compromise between simplicity and generality is to consider that, in age-structured populations, resources only affect the probability of survival of the reproductive age classes. Under these conditions, we can write a resource dependent model in the generic form, [31],

$$\begin{pmatrix} N_1^{n+1} \\ N_2^{n+1} \\ N_3^{n+1} \\ \vdots \\ N_k^{n+1} \end{pmatrix} = \begin{pmatrix} 0 & e_2 & e_3 \cdots & e_{k-1} & e_k \\ \alpha_1(R^n) & 0 & 0 \cdots & 0 & 0 \\ 0 & \alpha_2(R^n) & 0 \cdots & 0 & 0 \\ \vdots & \vdots & \vdots \cdots & \vdots & \vdots \\ 0 & 0 & 0 \cdots & \alpha_{k-1}(R^n) & 0 \end{pmatrix} \begin{pmatrix} N_1^n \\ N_2^n \\ N_3^n \\ \vdots \\ N_k^n \end{pmatrix} \qquad (29)$$
$$R^{n+1} = f(R^n)\phi(N^n)$$

where we have introduced a dynamic for the resources, and $N^n = N_1^n + \cdots + N_k^n$ is the total number of individuals in the population at time n. We also assume that the fertility coefficients are resource independent, which must be understood as an oversimplification.

To analyse the dynamical properties of map (29), we make some assumptions on the form of the functions $\alpha_i(R)$, $f(R)$ and $\phi(N)$. In order to derive general properties about the asymptotic states of the population numbers, we establish plausible limiting behaviours for the model functions, without specifying any particular functional forms for $\alpha_i(R)$, $f(R)$ and $\phi(N)$. The function $f(R)$ describes the dynamics of the resources alone through the iteration $R^{n+1} = f(R^n)$. We further assume that the resource map, $R^{n+1} = f(R^n)$, has a stable fixed point for $R^n = K$ and an unstable fixed point for $R^n = 0$.

We further assume that both $\alpha_i(R)$ and $f(R)$ are non-negative and monotonic increasing functions of R, and $\phi(N)$ is non-negative and monotonic decreasing func-

tion of N. Therefore, we have the following limiting values,

$$\begin{array}{l} \alpha_i(R) \to 0, \text{ as } R \to 0 \\ \alpha_i(R) \to 1, \text{ as } R \to \infty \\ f(R) \to 0, \text{ as } R \to 0 \\ \phi(N) \to 1, \text{ as } N \to 0 \\ \phi(N) \to 0, \text{ as } N \to \infty \end{array} \tag{30}$$

Under these conditions, it can be proved that ([31]):

Theorem 2: The map (29) together with conditions (30) is a diffeomorphism in the interior of the set $B = (N_1 \geq 0, \ldots, N_m \geq 0, R > 0)$. The resource dependent inherent net reproductive number $G(K) = \sum_{i=2}^{k} e_i \prod_{j=2}^{i} \alpha_{j-1}(K)$ is a bifurcation parameter for map (29). If $G(K) > 1$, but $G(K)$ is close to the value 1, then the map (29) has a non-zero stable fixed and is structurally stable in the interior of B.

The importance of Theorem 2 relies on the statement that the resources control the structural stability of model map (29), in the sense that any small perturbations of the map will not destroy the stability of the non-zero fixed point. Moreover, the structural stability result is independent of the functional form of $\alpha_i(R)$, $f(R)$ and $\phi(N)$.

In order to better understand the dynamic properties of map (29), we take a prototype model with three age classes, and we choose plausible functions $\alpha_i(R)$, $f(R)$ and $\phi(N)$. For the resources, we choose a logistic growth function,

$$f(R^n) = \frac{K\beta R^n}{R^n(\beta - 1) + K} \tag{31}$$

where $\beta \geq 1$ is the discrete time intrinsic growth rate, and K is the carrying capacity. Function (31) is a logistic type growth function for the resources and follows from (3), with $t = \Delta t$ and $\beta = e^{r_0 \Delta t}$. For the probability of survival between age classes, we assume that it has the form of a birth-and-death (stochastic) process, [32],

$$\alpha_i(R^n) = \frac{\gamma_i R^n}{\gamma_i R^n + 1} \tag{32}$$

where the $\gamma_i > 0$ are parameters. As γ_i becomes large, the probability of survival in the transition between consecutive age classes becomes close to 1, and $\alpha_i(R^n)$ becomes sensitive to the variations of resources only for small values of R^n (few available resources). The function $\phi(N)$ is assumed to have the Poisson form,

$$\phi(N^n) = e^{-N^n} \tag{33}$$

With $k = 3$, and introducing (31)-(33) into (29), we obtain the resource depen-

dent map,

$$\begin{pmatrix} N_1^{n+1} \\ N_2^{n+1} \\ N_3^{n+1} \end{pmatrix} = \begin{pmatrix} 0 & e_2 & e_3 \\ \dfrac{\gamma_1 R^n}{\gamma_1 R^n + 1} & 0 & 0 \\ 0 & \dfrac{\gamma_2 R^n}{\gamma_2 R^n + 1} & 0 \end{pmatrix} \begin{pmatrix} N_1^n \\ N_2^n \\ N_3^n \end{pmatrix} \tag{34}$$
$$R^{n+1} = \frac{K\beta R^n}{R^n(\beta - 1) + K} \exp\left(-(N_1^n + N_2^n + N_3^n)\right)$$

The phase space of map (34) has dimension 4. However, to analyze the bifurcation diagrams of the number of individuals, we simply plot the total number of individuals of the population, $N^n = N_1^n + N_2^n + N_3^n$, as a function of the control parameters. In Fig. 15, we show the bifurcation diagram for the total number of individuals calculated from map (34), as a function of the control parameter e_2. The other parameters have been fixed to the values $e_3 = 0.8$, $\gamma_1 = \gamma_2 = 1$, $K = 100$ and $\beta = 1000$.

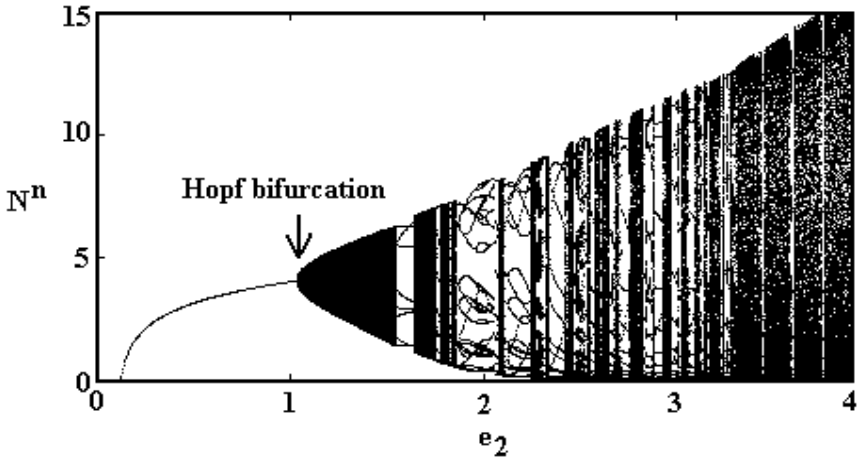

Fig. 15. Bifurcation diagram of map (34) for the parameter values $e_3 = 0.8$, $\gamma_1 = \gamma_2 = 1$, $K = 100$ and $\beta = 1000$, [31].

For, $0.11 < e_2 < 1.04$, the map (34) has a non-zero stable fixed point. Increasing e_2, this fixed point becomes unstable. The instability of the fixed point is due to a discrete Hopf bifurcation, and an invariant circle in phase space appears, [33], Fig. 15. The discrete Hopf bifurcation occurs when two complex conjugate eigenvalues of the Jacobian matrix of (34) evaluated at the period-1 fixed point cross the unit circle in the complex plane. On the invariant circle, the time evolution is not periodic anymore, and any time series or orbit becomes quasi-periodic. Increasing further the control parameter, there is a continuous region in the parameter space where regions of invariant circles in phase space and regions of periodic behaviour

appear. These regions are separated by bifurcations from quasi-periodic to periodic attractors (saddle-node discrete bifurcations) characteristic of circle maps, [33].

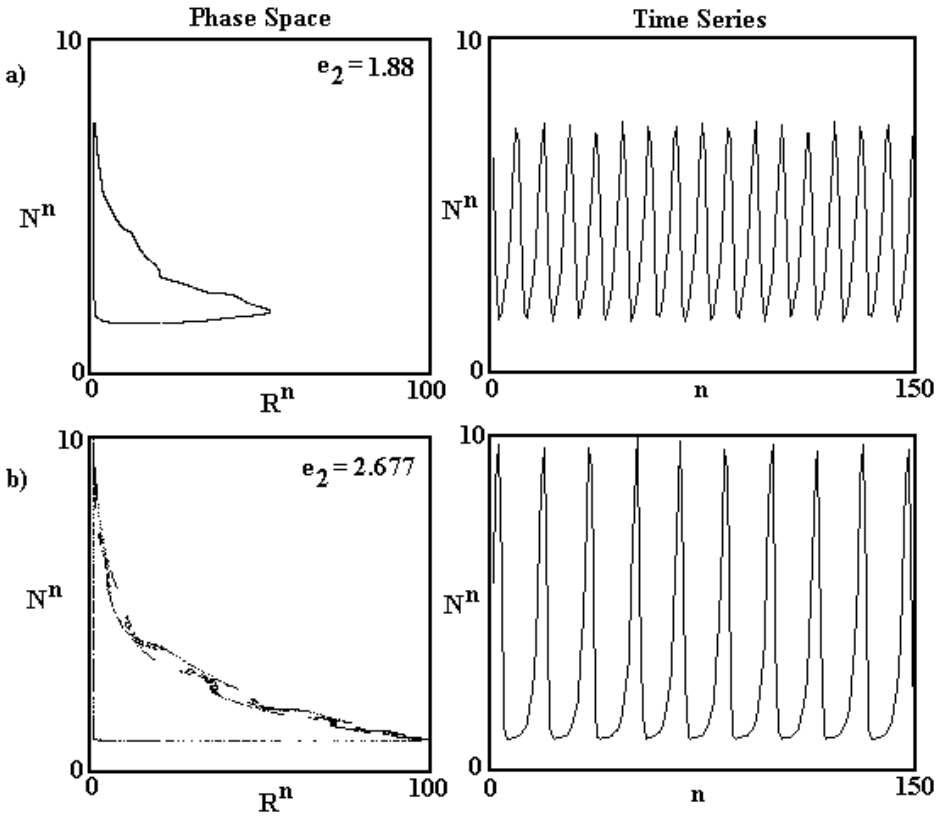

Fig. 16. Invariant sets in phase space and time series for map (34), for several values of the control parameter e_2. In a), the invariant set in phase space is homeomorphic to a circle, and in b) it is similar to a fractal set. In both cases, the corresponding time series are quasi-periodic. The time series of these quasi-periodic motions should be compared with the chaotic time series of Fig. 14.

In Fig. 16, we show the attractors and the time series for two different values of the parameter e_2. In Fig. 16a), the invariant trajectory in phase space is homeomorphic to a circle and has a quasi-periodic time series. In Fig. 16b), the invariant circle is destroyed and an invariant set appears, apparently, with a fractal structure. In this case, the quasi-periodicity of the time series is maintained. Further numerical analysis for other parameter values leads the conclusion that the random behaviour found in this map has a different characteristic than the one found in the chaotic case of the previous section.

Quasi-periodic time series have random behaviour. In fact, there exists a continuous probability distribution characterizing the permanence time of the iterates

of the map on the attractor in phase space, [34]. This probability distribution also exists in the chaotic maps (27) and (28). The difference between map (34) and maps (27) and (28) is that, in map (34), the phase trajectories on the invariant set have no unstable periodic orbits, whereas in chaotic systems invariant sets contain an infinite number of unstable periodic orbits. In both cases, the trajectories on the invariant sets are random because they are ergodic, leaving invariant the above-mentioned probability distribution, with support on the attractor. The time series of the chaotic system is clearly irregular, contrary to the quasi-periodic case where it is almost regular, despite the apparent similarities of bifurcation diagrams.

There is one more important distinction between the map (34) and the maps (27) and (28). The map (34) is a diffeomorphism in the positive part of phase space, and maps (27) and (28) are not invertible. Prototype models of chaotic dynamics are in general non-invertible. The map (34) becomes non-invertible in the limit $\beta \to \infty$. In this limit, we obtain, for the resource dynamics, $R^{n+1} = Ke^{-(N_1^n+N_2^n+N_3^n)}$. This corresponds to the introduction of a fast recovery time of the resources when compared with the time scale of the population. In this case, the structure of the invariant sets in phase space becomes more complex than the ones depicted in Fig. 16, and we observe regions of quasi-periodic behaviour mixed with regions with more complex time series, [31].

From the comparison between the models (27), (28) and (34), the main conclusion we want to point out is that, for hypothetical populations following these dynamics, the information provided by the bifurcation diagrams is not enough to decide about the degree of complexity of a time series. The structure of the attractors in phase space has to be taken into account. In principle, any analytical strategy in order to calibrate and validate models with chaotic or quasi-periodic behaviour in time must elucidate about the topological structure of the attractors and about fixed points in phase space.

7. Spatial effects

In general, in the search of resources or simply to avoid overcrowding, populations spread along space. In some species, the spreading is short-range and in others it has a long-range effect. In order to describe both effects in a simple formalism, we take the simplest case where the population at time $n+1$ relates to the population at time n, through the difference equation,

$$N^{n+1} = f(N^n) \tag{35}$$

where f is some arbitrary function, and N^n is the number of individuals in the population at time n. To introduce the effect of spatial spreading into (35), we let $N^n \equiv N^n(x)$, and the total population is,

$$\int_a^b N^n(x)dx = N_{tot}^n \tag{36}$$

where a and b define the limits of the territory. The limiting cases $a = -\infty$ and $b = +\infty$ are allowed. Now, $N(x)$ is the number of individuals of the population per unit of length or area. The spatial spreading effect is introduced into (35) by a dispersion kernel $k(y-x)$, and the local dynamics becomes,

$$N^{n+1}(x) = \int_a^b k(y-x) f(N^n(y)) dy \tag{37}$$

where, to avoid spatial asymmetries, we assume that $k(\cdot)$ is an even function of its argument. We impose further that,

$$\int_a^b k(z) dz = 1 \tag{38}$$

With condition (38), the kernel function $k(z)$ can be understood as a probability distribution, and the term $k(y-x)f(N^n(y))$ in (37) is the frequency of individuals that were at y at time n and will be at x at time $n+1$. Introducing, $z = y - x$ into (37), we obtain,

$$N^{n+1}(x) = \int_a^b k(z) f(N^n(z+x)) dz \tag{39}$$

The integro-difference equation (39) describes the time evolution of the density of individuals in the population and, depending of the form of the kernel function, it accounts for short- and long-range spreading effects.

In order to describe only short-range effects, we develop $f(N^n(z+x))$ in Taylor series around $z = 0$, and from (39), we obtain,

$$N^{n+1}(x) = f(N^n(x)) + D\frac{\partial^2}{\partial x^2}(f(N^n(x))) + \dots \tag{40}$$

where we have used the normalization condition (38), and,

$$D = \int_a^b k(z) z^2 dz \tag{41}$$

is the diffusion coefficient or second moment of the kernel function $k(z)$. The kernel function $k(z)$ is specific to the species under consideration, and, in principle, is related with the mobility of the population. Obviously, D is also species dependent. In [15] and [35], some examples of kernel functions used in ecological modelling are discussed.

We apply now this formalism to the study of the dispersal of a hypothetical population that follows a Ricker type dynamics (Sec. 5). Introducing the Ricker map (27) into the integro-difference equation (39), we obtain,

$$N^{n+1}(x) = r\int_{-\infty}^{+\infty} k(z) N^n(z+x) e^{-N^n(z+x)} dz \tag{42}$$

and we chose as dispersion kernel the normalized Gaussian function,

$$k(z) = \frac{1}{2\sqrt{\pi D}} e^{-z^2/4D} \tag{43}$$

where D is the diffusion coefficient.

To follow in time and space the growth of this hypothetical population, we consider a one-dimensional infinite domain with the initial density distribution,

$$N^0(x) = \begin{cases} 2 & \text{if} \quad |x| \leq 1 \\ 0 & \text{if} \quad |x| > 1 \end{cases} \tag{44}$$

By (36), the initial total population described by (44) has four individuals.

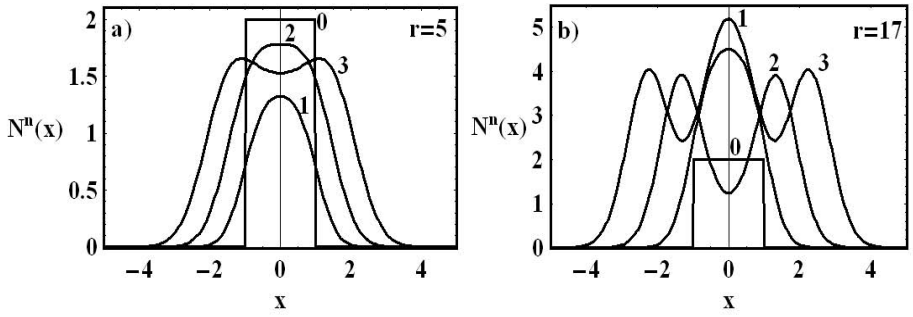

Fig. 17. First iterates of the integro-difference equation (42) associated to the Ricker map, for $D = 0.1$, (a) $r = 5$ and (b) $r = 17$. $N^n(x)$ is the density of individuals at the spatial region x and time n. The initial condition at time zero is given by (44). The numbers in the graphs represent the iteration time n.

To follow the space and time evolution of the number of individuals in the population, we introduce (44) into (42), and we iterate (42) for several values of the growth rate parameter r. In Fig. 17, we show the first iterates of the integro-difference equation (42), for the initial condition (44), and parameter values: $D = 0.1$ and $r = 5$; $D = 0.1$ and $r = 17$. For these parameter values, the Ricker map (27) has periodic and chaotic behaviour (Fig. 13), respectively. After four iterations, the total population numbers are: $N^4_{tot} = 9.6$, for $r = 5$, and $N^4_{tot} = 21.2$, for $r = 17$. In both cases, the initial condition corresponds to $N^0_{tot} = 4$.

The numerical simulations in Fig. 17a) show the formation of a dispersal front. Initially, the front amplitude has small oscillations. After some time, the front amplitude stabilizes and its value equals the value of the fixed point of the Ricker map (27). The front propagates in space and the population number increase in time. When $n \to \infty$, then $N^n \to \infty$. In Fig. 17b), the Ricker map has chaotic behaviour, and a dispersion front appears as time increases. In this case, at each point of the spatial region, the oscillations of the population density during time are chaotic, Fig. 18.

In Fig. 18a), we show, for the Ricker map (27), the time evolution of $N^n(0)$, calculated with the integro-difference equation (42). The time series at a given point of the extended system has the same type of chaotic behaviour as the time series obtained with Ricker map. In Fig. 18b), we show the graph of the points

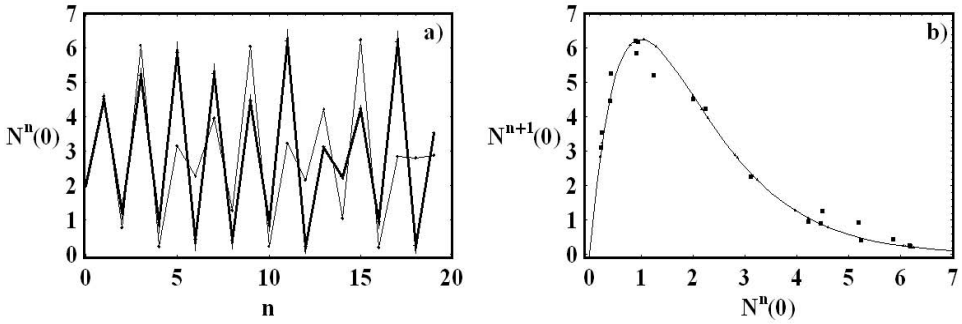

Fig. 18. a) The heavy line is the time series of the first iterates of the density of individuals $N^n(0)$, calculated with the integro-difference equation (42), for the Ricker map (27). The parameters values are, $D = 0.1$, $r = 17$, and the initial condition is given by (44) . The thin line is the iterate of the Ricker map, for the same parameter values, and the initial condition $N^0 = 2$. For these parameter values, the Ricker map is chaotic. As it is clearly seen from the time series, the chaotic behaviour is still present in the extended system. In b), we show the graph of the function $N^{n+1} = f(N^n) = rN^n e^{-N^n}$ (thin line), and the points $(N^{n+1}(0), N^n(0))$ from the time series in a). The iterates of the Ricker map are on the graph of the function $f(N^n)$ (triangles). The points $(N^{n+1}(0), N^n(0))$ obtained from the time series of the extended system are near to the graph of the function $f(N^n)$ (squares).

$(N^{n+1}(0), N^n(0))$. Also, in the extended system, the chaotic behaviour of the local map persists. In real extended systems, this effect gives information about the chaoticity or periodicity of the local dynamics.

This simple example shows that the dispersal effect strongly increases the equilibrium values of the population, implying that the dimension of the territory of a population is a constraining factor for the population growth. Note that, the Ricker map only admits finite values for the number of individuals of a population.

Suppose now that we have a population evolving according to the logistic equation (2), and we want to take into account dispersal effects. Applying to the logistic equation the same reasoning leading to the integro-difference equation (39), we obtain,

$$\frac{\partial N}{\partial t} = \int_a^b k(z) r N(z+x,t)(1 - N(z+x,t)/K) dz \tag{45}$$

together with the normalization condition (38). In this case, we obtain an integro-differential time evolution equation. To analyse short-range dispersal effects, by (40), we have,

$$\frac{\partial N}{\partial t} = rN(1 - N/K) + rD\frac{\partial^2}{\partial x^2}\left(N(1 - N/K)\right) \tag{46}$$

which is a parabolic partial differential equation.

We take the simple equilibrium solution of the logistic equation, $N(x) = K$. Introducing this solution into (46), $N(x) = K$ is a stationary solution of the parabolic equation (46). Therefore, by (36), the logistic model with dispersal admits an infinite

population in an infinite territory. Once more, it is clear that population numbers are dependent of the dimensions of the territory.

In the literature of ecology, dispersion effects are analysed through the parabolic equation,

$$\frac{\partial N}{\partial t} = rN(1 - N/K) + D\frac{\partial^2 N}{\partial x^2} \tag{47}$$

which is known as the Kolmogoroff-Petrovskii-Piskunov or Fisher equation. This equation is in general derived under the assumption of Fick laws that asserts that migration occurs from regions with higher densities to regions with lower densities. One of the properties of the solutions of the equation (47) is the possibility of having a propagating front along space, [36] and [37], analogous to the fronts of Fig. 17a).

To incorporate dispersion effects into continuous models of population dynamics, we can follow the reasoning leading to equations (45) and (46), or adopt the view leading to equation (47), introduced by Kolmogoroff-Petrovskii-Piskunov, [36]. In the last case, this corresponds to add a diffusive term, transforming the differential equations into a quasi-linear parabolic partial differential equation. Most of these spatial models are non-linear and their space and time solutions are found numerically. In references [15] and [35], several models with spatial effects are analysed.

8. Age-structured density dependent models

In the literature of ecology, density dependent models appear in several contexts. In the Leslie approach, the effects on population density can be introduced through the dependence of the probability of survival between age classes on the population numbers. In this case, the survival probabilities between the age classes are of the form $\alpha_i(N^n)$, where N^n is the total population at time n, [38], and the general non-linear map obtained falls in the class of non-linear maps of section 5. Also, in the previous section, we found a density dependent model in the sense that the state variable of the population has the generic form $N(x)$, representing the number of individuals by unit of area or length. All these models are, in a certain sense, density dependent. Here, we are interested in density dependent models where the age and time variables have a continuous nature, [39], [23], [40] and [41].

We consider a population age density function $n(a,t)$ such that,

$$N(t) = \int_0^{+\infty} n(a,t)da \tag{48}$$

where $N(t)$ is the total population at time t, and a represents age. The function $n(a,t)$ is the density of the individuals of the population with age a at time t. The births are described by the fertility function by age class $b(a,t)$, and are given by,

$$n(0,t) = \int_0^{+\infty} b(a,t)n(a,t)da \tag{49}$$

Assuming that the normalised death rate of the density of individuals (mortality modulus) of the population is constant (μ), we have,

$$\frac{dn}{dt} = -\mu n \tag{50}$$

As aging is time dependent, $a \equiv a(t)$, and is measured in the same time scale of time, $\frac{da}{dt} = 1$, by (50), the function $n(a(t), t)$ obeys the first order linear partial differential equation,

$$\frac{\partial n(a,t)}{\partial t} + \frac{\partial n(a,t)}{\partial a} = -\mu n(a,t) \tag{51}$$

together with the boundary condition (49). Equation (51) is the McKendrick equation, [39].

Let us find now a solution of the McKendrick partial differential equation (51) by elementary geometric methods. Writing equation (51) in the form, $\frac{dn(a,t)}{dt} = -\mu n(a,t)$, where a is also a function of t, the solutions of (51) are obtained through the solutions of the system of ordinary differential equations,

$$\begin{cases} \frac{dn}{dt} = -\mu n \\ \frac{da}{dt} = 1 \end{cases} \tag{52}$$

These two independent equations have the general solution,

$$\begin{cases} n(a,t) = n(a_0, t_0)e^{-\mu(t-t_0)} \\ a - a_0 = t - t_0 \end{cases} \tag{53}$$

where a_0 is the continuous age variable for $t = t_0$. The second equation in (53) is the equation of the characteristic curves of the partial differential equation (51), Fig. 19. Introducing the second equation in (53) into the first one, we obtain the solution of the McKendrick equation,

$$n(a,t) = n(a-t, 0)e^{-\mu t}, \quad \text{for} \quad t < a \tag{54}$$

where $n(a, 0)$ is an initial density distribution of the population at $t_0 = 0$. For $t < a$, the solution (54) is independent on the boundary condition (49). The domain of the solution (54) is the region labelled with a zero in Fig. 19.

To extend the solution (54) for $t \geq a$, the boundary condition must be introduced, as well as some additional simplifications. We suppose that births occur at some unique fixed age $a = a_1$, Fig. 19. Then, the fertility function is necessarily concentrated at the point $a = a_1$. Therefore, as fertility function by age class, we take,

$$b(a,t) = b\delta(a - a_1)$$

where $\delta(\cdot)$ is the Dirac delta function and b is a (mean) fertility parameter. Under these conditions, the boundary condition (49) simplifies to,

$$n(0,t) = bn(a_1, t) \tag{55}$$

We extend now the solution (54) to $t = a$, with the boundary condition (55). By (53) and (55), the solution of the McKendrick equation (51) is,

$$n(a,t) = n(0,0)e^{-\mu t} = bn(a_1,0)e^{-\mu t}, \quad \text{for} \quad a = t \tag{56}$$

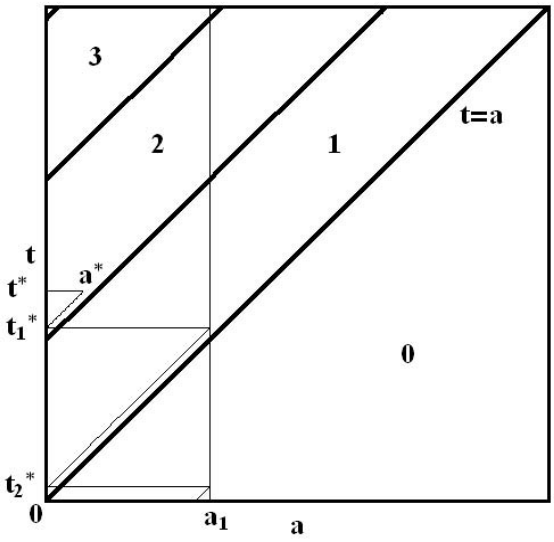

Fig. 19. Characteristic curves $a - a_0 = t - t_0$ for the McKendrick equation (51). The graph of the characteristic curves lies in the domain of the solution $n(a,t)$. Given an arbitrary point (a^*, t^*) in the domain of the partial differential equation, the solution $n(a^*, t^*)$ is easily obtained following the thin line backwards in time down to $t = 0$. The heavy lines are characteristic curves defined by the equations $t = a + ma_1$, for $m = 0, 1, \ldots$.

With a simple geometric construction, we calculate now the solution for $t > a$. We take the point (a^*, t^*) on the line $t = t^*$, Fig. 19. This point is in the region labelled 2 in Fig. 19. By (53), the characteristic line that passes by (a^*, t^*) crosses the line $a = 0$ at some time $t = t_1^*$, and $n(a^*, t^*) = n(0, t_1^*)e^{-\mu(t^* - t_1^*)} = n(0, t^* - a^*)e^{-\mu(t^* - t_1^*)}$, where $t_1^* = t^* - a^*$. Imposing on this solution the boundary condition (55), we obtain, $n(a^*, t^*) = bn(a_1, t^* - a^*)e^{-\mu(t^* - t_1^*)}$. As $n(a_1, t^* - a^*)$ is the solution of the McKendrick equation at the point $(a_1, t^* - a^*)$, we repeat the above construction, by drawing the horizontal line connecting the points $(0, t_1^*)$ with (a_1, t_1^*), Fig. 19. Iterating this procedure backwards in time, we obtain,

$$\begin{aligned} &n(a^*, t^*) = b^2 n(a_1, t^* - a^* - a_1)e^{-\mu(t^* - t_1^* + t_1^* - t_2^*)} \\ &= b^2 n(2a_1 + a^* - t^*, 0)e^{-\mu(t^* - t_1^* + t_1^* - t_2^* + t_2^* - 0)} \\ &= b^2 n(2a_1 + a^* - t^*, 0)e^{-\mu t^*} \end{aligned} \tag{57}$$

where $t_2^* = t^* - a_1^* - a^*$, and we systematically have used the equation of the characteristic curves, $a - a_0 = t - t_0$. In Fig. 19, for any initial condition inside the

region labelled with an integer, say m, an easy induction argument shows that the solution of the McKendrick equation (51) has the form (57), where the factor 2 is substituted by m, where $m = [(t-a)/a_1 + 1]$ and $[x]$ stands for the integer part of x. Then, by simple geometric arguments, we have proved:

Theorem 3: Let $n(a,0)$ be an initial data function for the McKendrick partial differential equation (51), with $a \geq 0$, $t \geq 0$ and $\mu > 0$. Then, for the boundary condition (55), with a_1 and b positive constants, the general solution of the McKendrick partial differential equation is,

$$\begin{aligned} &n(a,t) = n(a-t,0)e^{-\mu t}, \quad \text{for} \quad t < a \\ &n(a,t) = b^{[(t-a)/a_1+1]} n([(t-a)/a_1 + 1]\, a_1 + a - t, 0)e^{-\mu t}, \quad \text{for} \quad t \geq a \end{aligned} \tag{58}$$

where $[x]$ stands for the integer part of x.

We analyse now the stability of the solution (58) of the McKendrick partial differential equation. As $[(t-a)/a_1] + 1 = m$, where m is a positive integer, we have, $(t-a)/a_1 + 1 = m + \varepsilon(a,t)$, and, for fixed a, with $t \geq a$, the function $\varepsilon(a,t)$ is time periodic with period a_1. Therefore,

$$b^{[(t-a)/a_1+1]} e^{-\mu t} = e^{[(t-a)/a_1](\ln b - \mu a_1)} b e^{-\mu a} e^{-\mu a_1 \varepsilon(a,t)}$$

By (58), and for $t \geq a$, we have,

$$n(a,t) = e^{[(t-a)/a_1](\ln b - \mu a_1)} n([(t-a)/a_1 + 1]\, a_1 + a - t, 0) b e^{-\mu a} e^{-\mu a_1 \varepsilon(a,t)} \tag{59}$$

Then, if $(\ln b - \mu a_1) = 0$, the asymptotic solution of the McKendrick partial differential equation is periodic in time. If, $b > e^{\mu a_1}$, asymptotically in time, the population density goes to infinity, and if, $b < e^{\mu a_1}$, the population density goes to zero. Hence, we have:

Corollary 4: *Let $n(a,0)$ be a differentiable and bounded initial data function for the McKendrick partial differential equation (51), with boundary condition (55). Suppose in addition that $\ln b = \mu a_1$. Then, the asymptotic solution of the McKendrick equation is bounded and periodic in time, with period a_1:*

$$n(a,t) = n([(t-a)/a_1 + 1]\, a_1 + a - t, 0) b e^{-\mu a} e^{-\mu a_1 \varepsilon(a,t)}$$

In Fig. 20, we show the time evolution of an initial population with an uniform age distribution, with a maximal age class, and obeying to the stability condition $b = e^{\mu a_1}$. We have chosen for initial conditions the density function: $n(a,0) = 2$, for $a \leq 100$, and $n(a,0) = 0$, for $a > 100$. By (48), this corresponds to the initial population, $N(0) = 200$. The calculated population numbers for $t = 30$ and $t = 100$ are $N(30) = 110.7$ and $N(100) = 70.9$, respectively. As it is clearly seen in Fig. 20, after a transient time, the population density becomes periodic in time, as asserted in Corollary 4.

In Fig. 21, we show the total population as a function of time, calculated from Theorem 3 and (48), with the initial condition and parameters from Fig. 20. In

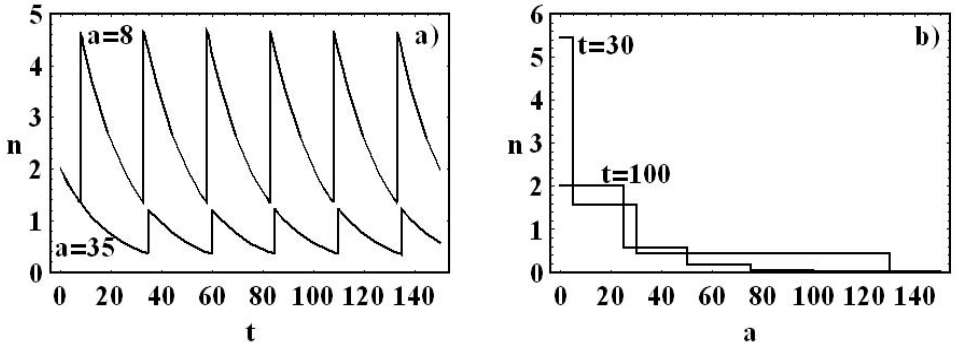

Fig. 20. a) Time evolution of the solution of the McKendrick equation (51), for the age classes $a = 8$ and $a = 35$. b) Distribution of the number of individuals by age class, for $t = 30$ and $t = 100$. All these solutions have been calculated with the initial data condition, $n(a, 0) = 2$, for $a \leq 100$, and $n(a, 0) = 0$, for $a > 100$, and parameter values, $a_1 = 25$ (unique reproductive age class), $\mu = 0.05$ (death rate) and $b = e^{\mu a_1} = 3.49$ (mean fertility).

the McKendrick continuous age-structured approach, the asymptotic stable state of the dynamics are not fixed points as in the case of the Leslie type maps (Sec. 3), but bounded time periodic function. Moreover, by Theorem 3, the amplitude of oscillations depends on the initial data function $n(a, 0)$.

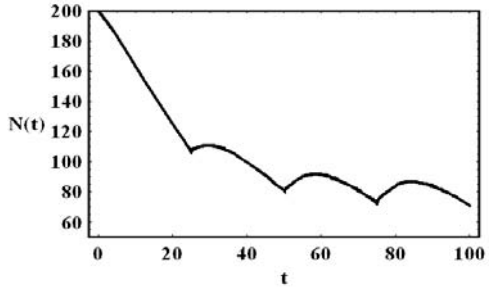

Fig. 21. Total population as a function of time, for the same parameter values of Fig. 20. After a transient time, the period of oscillations is a_1, the age of the unique reproductive age class.

If, $b > e^{\mu a_1}$, by (59), it can be shown that the growth curve is modulated by a time periodic function with period a_1, [42]. For two reproductive age classes and boundary condition $n(0, t) = b_1 n(a_1, t) + b_2 n(a_2, t)$, the growth curves are always modulated by two time periodic functions with periods a_1 and a_2. If these periods are not rationally related ($n_1 a_1 + n_2 a_2 = 0$, has no integer solutions in n_1 and n_2), the modulation function is quasi-periodic. In the population dynamics literature the quasi-periodic modulations of the growth curves are called demography cycles. For a detailed discussion see [42].

In the more general case of age dependent fertility function and mortality modulus, $b(a)$ and $\mu(a)$, the qualitative behaviour and stability properties of the solutions of the McKendrick equation (51) are determined by the Lotka growth rate, [24] and [42],

$$r = \int_{a_1}^{a_2} b(c) e^{-\int_0^c \mu(s) ds} dc \tag{60}$$

where a_1 and a_2 are the ages of the first and the last reproductive age classes, and $b(a)$ and $\mu(a)$ are determined from demography data.

To estimate the growth of populations, the Lotka growth rate is an important demography tool, [25]. A detailed analysis shows that, the discrete approximation of (60) coincides with the inherent net reproductive number of a population (21), [42], introduced in the discrete time and age Leslie formalism of Sec. 3.

We can now compare the solution of the McKendrick equation derived in Theorem 3 with the exponential solution of the Malthusian growth model (1). Assuming that $t \geq a$, we have, $n(a, t + sa_1) = n(a, t)r^s$, where s is an integer and $r = be^{-\mu a_1}$ is the Lotka growth rate. With $t = a_1$ and $\tau = a_1 + sa_1$, we obtain, $n(a, \tau) = n(a, a_1)r^{(\tau - a_1)/a_1}$. Integrating $n(a, \tau)$ in a, we have for the total population,

$$N(\tau) = N(a_1)r^{(\tau - a_1)/a_1}$$

which is a Malthusian growth function with Lotka growth rate r. Therefore, with a time step equal to the age of the only reproductive age class (a_1), the solution of the McKendrick equation behaves like the exponential growth model of Sec. 2.

9. Growth by mitosis

When reproduction occurs by mitosis as in cells and some micro-organisms, the growth model of the previous section must be modified. We consider a population of micro-organisms or cells in a media with enough resources, eventually infinite. We assume that the micro-organisms replicate by mitosis, and the time of the mitotic processes can be neglected. We represent by $n(a, t)$ the density of organisms in the media with age a at time t.

We consider that the probability of dying depends only on the age. We denote by $\mu(a)$ the probability density of death with age a, and $b(a)$ is the probability density of undergoing mitosis with age a . If an organism initiates mitosis, then, after some time, the organism transforms into two new ones with age zero. Therefore, the density of newborns at time t is,

$$n(0, t) = 2 \int_0^\infty b(a) n(a, t) da \tag{61}$$

where the factor 2 accounts for the mitotic process.

Hence, the time evolution of the colony of micro organisms is described by the modified McKendrick equation,

$$\frac{\partial n(a,t)}{\partial t} + \frac{\partial n(a,t)}{\partial a} = -\left(\mu(a) + b(a)\right) n(a,t) \tag{62}$$

together with the boundary condition (61).

We consider a population where all the individuals initiate mitosis at some fixed age $a = \alpha$, such that $b(a) = \delta(a - \alpha)$. To simplify even further, we suppose that $\mu(a) = \mu$ is constant, independently of the age. So, by (60), (61) and (62), the Lotka growth rate is now,

$$r = 2\int_0^\infty \delta(a-\alpha) e^{-\int_0^a (\mu(s) + \delta(s-\alpha))ds} da \tag{63}$$

As,

$$\int_0^a \delta(s-\alpha)ds = \begin{cases} 0, & \text{if } a < \alpha \\ 1/2, & \text{if } a = \alpha \\ 1, & \text{if } a > \alpha \end{cases} \tag{64}$$

by (64) and (63), for a population with mitotic reproduction type, the Lotka growth rate is,

$$r = 2e^{-\mu\alpha} e^{-1/2} \tag{65}$$

Making $\mu = 0$ in (65), for the Lotka growth rate, we obtain the constant value,

$$r = 2e^{-1/2} = 1.21306$$

In the case of sexual reproduction and in the limit case of zero mortality, by (60), we have,

$$r = \int_{a_1}^{a_2} b(c)dc \tag{66}$$

which can be larger or smaller than 1, depending on the intrinsic fertility of the species. In mitosis, in the limiting case of zero mortality, the Lotka growth rate is always greater than 1, ensuring an exponential growth process. On the other hand, by (65), in organisms that reproduce by mitosis, r cannot take large values, but in the case of organisms with sexual reproduction, by (66), r can be arbitrary large.

The application of the McKendrick approach to the growth of colonies of micro-organisms is described in detail in Rubinow [43].

10. Conclusions

Along this review we have derived the most common models used in ecology and population dynamics. Differential and difference equation models, describe a population as whole, in the sense that they do not distinguish either intra-specific characteristics of the individuals, or their spatial distribution. The calibration of these

models with real biological situations is not always successful and, in the context of growth projections, they must be considered as toy models. However, the analysis of their dynamic behaviour introduced in the language of ecology new concepts that later were generalised to the age-structure approach. This is the case of the concept of growth rate, introducing a quantitative measure of the stability or instability of a population.

The dependence of the carrying capacity and of the growth rate parameters on the dimensions of the territories and on the available resources, is also an important issue. Experimental measurements of growth of micro-organisms as a function of resources has been done by Monod, [44].

The class of age-structured models gives us a more detailed insight on the dynamics of a population. In demography studies, the Leslie and the McKendrick approaches are nowadays the reference models. In the context of microbiology, the same structure and theoretical setting holds as it has been shown in Rubinow, [43]. One of the consequences of the age-structured McKendrick approach to the population growth is that, in a time scale of the order of the mean age of the reproductive classes, populations have a Malthusian type growth pattern with a Lotka growth rate. The Malthusian growth pattern is perturbed by periodic functions which globally induce quasi-periodic demography cycles.

The distinction between chaos and quasi-periodicity in real ecological systems, is not a simple subject. We have presented models based on the difference equations approach that are non-invertible and have chaotic behaviour. However their calibration with real biological systems presents some difficulties. Models showing quasi-periodicity are invertible, and the restriction to the phase space attractors make them similar to circle maps. Technically, both chaotic and quasi-periodic systems are ergodic, leaving invariant a probability measure. This property implies that chaotic and quasi-periodic systems have the same type of randomness.

In generic terms, the dynamical properties of chaotic and quasi-periodic systems are strongly dependent of the adopted mathematical models. The question whereas a basal population or a population at the top of a trophic chain follow any of these choices can only be verified by observation.

One possible way of distinguishing between chaos and quasi-periodicity in populations is through the analysis of the population dispersal. As it has been seen in section 7 for the dispersal of a population, the characteristics of the temporal dynamics is imprinted in the density profile along space. The analysis of this effect gives information about chaoticity or periodicity of the local dynamics.

Some of these models are sensitive to perturbations of the functional forms of the growth rates, others are not. For populations at the top or at the bottom of a trophic chain, it is difficult to conceive that growth models could be too sensitive to arbitrary small external factors. In this case, the structural stability property should be a mandatory property for the choice of any mathematical model for the population growth.

Table 1. Comparison between the properties of the population growth models analysed along the text. In the case of partial differential equation models, the concept of structural stability needs a different approach from the one explored here. Notes: 1) Structural stability refers to persistence upon perturbations of the non-zero equilibrium in phase space. 2) In mutualistic interactions we can have explosion of population numbers. This case has not been considered in this classification. 3) The zero equilibrium state is always unstable. 4) Technically, if the rotation number around the closed trajectories is irrational, the time series is quasi-periodic. 5) In general, the Leslie matrix has non dominant complex eigenvalues, introducing quasi-periodic modulations in the growth curves. 6) If the Leslie matrix has no eigenvalues on the unit circle of the complex plane, then the Leslie map is structuraly stable. 7) Chaos occurs for some of these models when the recovery time of the resources goes to zero, [31]. 8) The McKendrick model has quasi-periodic time behaviour in the sense that growth curves are modulated by periodic functions, with periods equal to the ages of the reproductive age classes, [42]. 9) In general, the concept of structural stability is not defined for partial differential equations.

Population growth model	Non-zero equilibrium	Population goes to ∞	Population dies out	Oscillations	Chaos	Quasi-periodicity	Structural stability (1)
Malthusian	no	yes	no	no	no	no	yes
Logistic	yes	no	no	no	no	no	yes
Logistic controlled by resources	no	no	yes	no	no	no	yes
Biotic interactions (Sec. 2.2)	yes	no (2)	no (3)	no	no	no	yes
Lotka-Volterra	yes	no	no	yes	no	yes (4)	no
Leslie	yes	yes	yes	yes (5)	no	yes (5)	yes (6)
Leslie controlled by resources	yes	no	yes	yes	yes (7)	yes	yes
Ricker	yes	no	yes	yes	yes	no	yes
McKendrick	no	yes	yes	yes	no	yes (8)	(9)

We have compared the dynamic properties of the models derived along this review. We have analysed the models according the possibility of describing population extinction and explosion, non-zero equilibrium states, oscillations, chaos and quasi-periodicity. The structural stability or robustness of the models in phase space is, in simple terms, related with the conditions of the Hartman-Grobman theorem (Theorem 1), and with the non-existence of phase space trajectories connecting unstable fixed points. For this global comparison, we have considered that growth rates are always positive. The properties of the analysed models are summarised in Table 1.

For all the models analysed along this review, it is evident that, the same biological assumptions, but different technical options, lead to different models with different properties, Table 1. The choice of the appropriate model to describe a specific living system must rely on the calibration and validation of the model results with the growth projections.

Some other modelling approaches to ecology and population dynamics were not focused in this review. This is the case of the dynamic energy budget approach, [45], topics related with resource exploration and eco-economics, [46], harvesting, [47] , [46] and [48], epidemics and dispersal of diseases, [15], [30] and [49]. In the dynamic energy budget approach, the main objective is to make an integrative view of the different levels of organization of biological systems, from simple micro-organisms to ecosystems. In the resource exploration aspects of ecology and eco-economics, concepts of economic theory are introduced in the framework of ecology. Harvesting models are important to analyse problems of control and over consumption of natural resources, [46]. Also, harvesting models are an alternative approach to describe predation in species that are incorporated in trophic webs, [48]. Epidemics and dispersal of diseases are important subjects due to its immediate application to health prevention issues. For a recent account on more specialised mathematical models in biological sciences see [50].

Acknowledgments

I would like to thank Professor J. C. Misra for his kind invitation to write an introductory review on mathematical modelling in ecology and population dynamics. This work has been partially supported by the PRAXIS XXI Project P/FIS/13161/1998 (Portugal), and by the Institut des Hautes Études Scientifiques (Bures-sur-Yvette, France).

References

1. S. H. Strogatz, Exploring complex networks, *Nature* **410** (2001) 268-276.
2. M. Braun, Single species population models. In *Differential Equations Models*, vol. 1, (Edited by M. Braun, C. S. Coleman and D. A. Drew), Springer-Verlag, New York, 1978.
3. H. G. Schlegel, *General Microbiology*, Cambridge Uni. Press, Cambridge (1993).

4. H. Haberl and H. P. Aubauer, Simulations of human population dynamics by a hyperlogistic time-delay equation, *J. Theo. Biol.* **156** (1992) 499-511.
5. G. F. Gause, *The Struggle for Existence*, Williams and Wilkins, New York (1934).
6. R. Dilão and T. Domingos, A general approach to the modelling of trophic chains, *Ecological Modelling* **132** (2000) 191-202.
7. A. I. Volpert, V. A. Volpert and V. A. Volpert, *Travelling Wave Solutions of Parabolic Systems*, American Math. Soc., Providence (1994).
8. F. M. Scudo and J. R. Ziegler, *The Golden Age of Theoretical Ecology: 1923-1940*, Lecture Notes in Biomathematics n^o 22, Springer-Verlag, Berlin (1978).
9. V. Volterra, *Leçons sur la Théorie Mathématique de la Lutte pour la Vie*, Gauthier-Villars, Paris (1931).
10. R. L. Coren, The Evolutionary Trajectory, Gordon and Breach, New York (1998).
11. J. Guckenheimer and P. Holmes, *Nonlinear Oscillations, Dynamical Systems, and Bifurcations of Vector Fields*, Springer-Verlag, Berlin (1983).
12. M. W. Hirsh and S. Smale, *Differential Equations, Dynamical Systems and Linear Algebra*, Academic Press (1974).
13. N. J. Gotteli, *A Primer of Ecology*, Sinauer Associates, Sunderland (1995).
14. R. M. May, *Stability and Complexity in Model Ecosystems*, Princeton Uni. Press, Princeton (1974).
15. J. D. Murray, *Mathematical Biology*, Springer-Verlag, New-York (1989).
16. C. S. Holling, The functional response of predators to prey density and its role in mimicry and population regulation, *Mem. Entomol. Soc. Canada* **45** (1965) 5-60.
17. L. A. Real, The kinetics of functional response, *The American Naturalist* **111** (1977) 289-300.
18. A. A. Berryman, The origins and evolution of predator-prey theory, *Ecology* **73** (1992) 1530-1535.
19. T. Royama, A comparative study of models for predation and parasitism, *Res. Popul. Ecol. Supp.* **1** (1971) 1-90.
20. P. H. Leslie, On the use of matrices in certain population mathematics, *Biometrika* **33** (1945) 183-212.
21. Instituto Nacional de Estatística-Portugal. Idicadores demográficos séries 1960–1999; Resultado definitivos, censos 1940, 1960, 1970, 1980 e1991; I-Movimento geral da população.
22. R. E. Mickens, *Difference Equations, Theory and Applications*, van Nostrand, New York (1990).
23. H. Caswell, *Matrix Population Models,* Inc. Publishers, Sunderland (1989).
24. J. M. Cushing, *An Introduction to Structured Population Dynamics*, SIAM, Philadelphia (1998).
25. N. Keyfitz and W. Flieger, *World Population Growth and Aging*, Uni. Chicago Press, Chicago (1990).
26. W. Ricker, Stock and recruitment, *J. Fish. Res. Board Canada* **11** (1954) 559-663.
27. R. M. May, Simple mathematical models with very complicated dynamics, *Nature* **261** (1976) 459-467.
28. R. F. Costantino, R. A., Desharnais and J. M. Cushing, Chaotic dynamics in an insect population, *Science* **275** (1997) 389-391.
29. C. Zimmer, Life after chaos, *Science* **284** (1999) 83-86.
30. R. H. MacArthur, *Geographical Ecology*, Princeton Uni. Press., Princeton (1972).
31. R. Dilão and T. Domingos, Periodic and quasi-periodic behavior in resource-dependent age structured population models, *Bull. Math. Biology* **63** (2001) 207-230.
32. N. T. J. Bailey, *The Elements of Stochastic Processes*, Wiley Interscience Publica-

tions, New York (1964).
33. Y. A. Kuznetsov, *Elements of Applied Bifurcation Theory*, Springer-Verlag, New York (1995).
34. V. I. Arnold and A. Avez, *Problèmes Ergodiques de la Mécanique Classique*, Gauthier-Villars, Paris (1967).
35. M. Kot, M. A. Lewis and P. Driessche, Dispersal data and the spread of invading organisms, *Ecology* **77** (1996) 2027-2042.
36. A. Kolmogoroff, I. Petrovskii and N. Piskunov, A study of the equation of diffusion with increase in the quantity of matter, and its application to a biological problem, Moscow Uni. Bull. Math. 1 (1937) 1-25. Reprinted in P. Pelc, Dynamics of Curved Fronts, Academic Press, Boston, pp. 105-130, 1988.
37. P. Grindrod, *Patterns and Waves*, Clarendon Press, Oxford (1991).
38. A. Wikan, Four-periodicity in Leslie matrix models with density dependent survival probabilities, *Theoretical Population Biology* **53** (1998) 85-97.
39. A. G. McKendrick, Applications of mathematics to medical problems, *Pro. Edinburgh Math. Soc.*, **44** (1926) 98-130.
40. G. Oster, and J. Guckenheimer, Bifurcation phenomena in population models. In *The Hopf Bifurcation and its Applications*, (Edited by J. E. Marsden and M. McCracken), Springer-Verlag, New York (1976).
41. A. M. Roos, A gentle introduction to physiologically structured population models. In *Structured-population models in marine, terrestrial, and freshwater systems*, (Edited by S. Tuljapurkar and H. Caswell), Chapman & Hall, New York (1996).
42. R. Dilão and A. Lakmeche, On the weak solutions of the McKendrick equation with time and age dependent birth rate, in preparation.
43. S. I. Rubinow, *Mathematical Problems in the Biological Sciences*, SIAM, Philadelphia (1973).
44. J. Monod, *Recherches sur la croissance des cultures bactriennes*. Hermann & Cie., Paris (1942).
45. S. A. L. M. Kooijman, *Dynamic and Energy Mass Budgets in Biological Systems*, Cambridge Uni. Press, Cambridge (2000).
46. C. W. Clark, *Mathematical bioeconomics*. Wiley InterScience, New York (1990).
47. J. R. Beddington and R. M. May, Harvesting natural populations in a randomly fluctuating environment, *Science*, **197** (1977) 463-465.
48. R. Dilão, T. Domingos and E. Shahverdiev, Harvesting in a resource dependent age structured Leslie type population model, *Mathematical Biosciences*, **189** (2004) 141-151.
49. N. M. Ferguson, M. J. Keeling, W. J. Edmunds, R. Gani, B. T. Grenfell, R. M. Anderson and S. Leach, Planning for smallpox outbreaks, *Nature*, **425** (2003) 681-685.
50. L. Chen, Y. Kuang, S. Ruan and G. Webb, Advances in Mathematical Biology, *Discrete and Continuous Dynamical Systems – Series B*, **4** (2004) 501-866.